INTRODUCTION TO COMPUTATIONAL FLUID DYNAMICS

Enrico Nobile

Dipartimento di Ingegneria e Architettura
Università degli Studi di Trieste, 34127 TRIESTE

March 2, 2025

OUTLINE

Part I

Overview

CFD

What is Computational Fluid Dynamics - CFD ?

- CFD – Computational Fluid Dynamics = CFD – Computational Fluid Dynamics + NHT – Numerical Heat Transfer;
- By CFD we mean the set of techniques, numerical and non-numerical, used for the approximate solution (prediction) of the motion of fluids and associated phenomena (heat exchange, mass exchange, combustion, chemical reactions, etc.);
- With CFD techniques, the solution of the differential (or integro-differential) equations that govern the phenomena (continuity, momentum, energy, etc.), is approximated through the discretization of the domain - spatial and temporal) - of interest:
  - The problem changes from continuous to discrete;
  - CFD is deeply linked to the existence and use of the computer.

CFD - *cont.*

- CFD can provide information on:
  - Distribution of velocity, pressure, temperatute et.
  - Forces (Lift, Drag);
  - Distribution of multiples phases (gas-liquid, gas-solid et.);
  - More...
- CFD and NHT can be used in different stages of the engineering process:
  - Initial conceptual (exploratory) studies;
  - Detailed product development;
  - Optimization;
  - Troubleshooting & redesign.
- CFD complements experimentation (at real-scale or model-scale) reducing overall costs, time, number of experimental prototypes et.
- In some particular circumstances - regulations, cost reduction (i.e. America's Cup) - CFD replaces physical testing.

CFD vs NFD

- Someone (Roache, 1976) distinguishes between *Computational Fluid Dynamics* (or, equivalently, *Numerical Simulation of Fluid Dynamics*) from the more general term *Numerical Fluid Dynamics*;
- By *Numerical Fluid Dynamics* we mean all numerical techniques applied to the solution of fluid dynamics problems (ordinary differential equations, characteristic method, etc.);
- Furthermore, with CFD we mean, in addition to the typical applications in the industrial sector, also the research activities associated with it (basic, applied and pre-competitive) aimed at methods (e.g. numerical methods), models (e.g. turbulence, combustion etc.) and applications.

CFD: multidisciplinary matter

Overview of the disciplines *contained* in CFD:

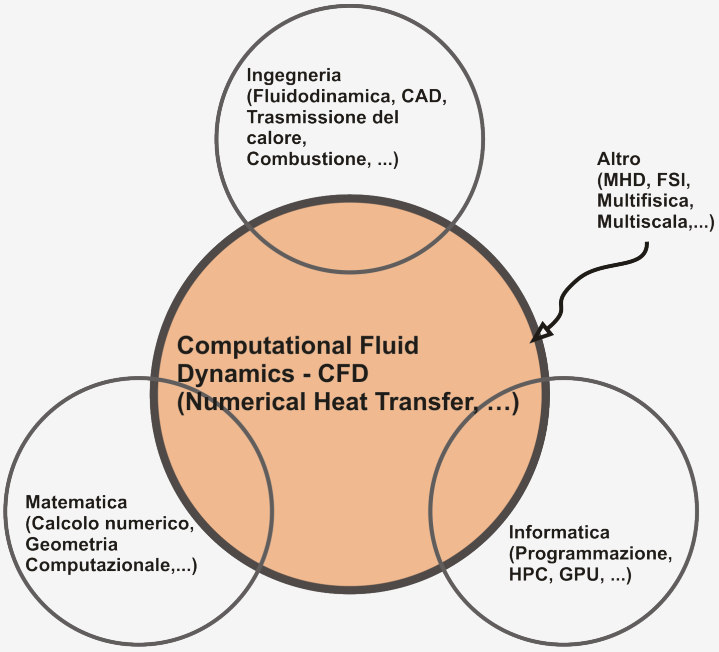

Brief historical notes

- CFD was originally born within large public and private research centers around the 1960s [Los Alamos: J. Von Neumann, 1950; Harlow and Welch (Physics of Fluids), 1965. IBM: Fromm J.E. (IBM J. Research and Development), 1971];
- Initially, it spread almost exclusively in the aeronautical and aerospace sectors (in-house codes);
- Subsequently, thanks to the continuous increase in the performance of computing platforms and the reduction of related costs, and to the development of commercial CFD packages, it has gradually spread in the academic field and in some industrial sectors (automotive, turbomachinery, energy, etc.);
- Its use is currently increasingly widespread, as a result of:
  - Availability of increasingly versatile and feature-rich commercial (industrial) CFD packages (models, ease of use, CAD integration, etc.);
  - Availability of Open Source libraries and packages;
  - Hardware with increasing performance and reduced costs (multi-core, clusters, GPUs etc.).
- The fields of application of CFD are numerous, and concern any discipline and/or problem in which the motion of fluids is of some interest;
- We can list them (1) by application sector and (2) by application.

Application areas

Un possibile elenco - non esaustivo - è il seguente:

- Basic and applied research;
- Educational activities;
- Aeronautics and aerospace sector;
- Automotive sector;
- Naval and off-shore sector;
- Railway sector;
- Electrical and electronic engineering;
- Bioengineering and medical;
- Chemical and process industry;
- Nanotechnology;
- Civil and environmental engineering;
- Energy sector (traditional, renewable sources, nuclear, fusion, etc.);
- Sports (Automotive, motorcycle, sailing, cycling, skiing, swimming, etc.);
- Safety (explosions, fires, etc.).

Applications

The possible applications are numerous, let's see some of them (non-exhaustive list):

- External aerodynamics (airplanes, cars, trains, motorbikes etc.);
- Free surface hydrodynamics (ships, boats);
- Fluid dynamics and combustion of internal combustion engines;
- Turbomachinery (pumps, compressors, hydraulic turbines, steam and gas turbines, wind generators);
- Heat transfer (heat exchangers, batteries, thermal control in microelectronics);
- Magnetofluid dynamics (brakes and electromagnetic *stirrers* in the production and continuous casting processes of metals);
- Naval propulsion systems, with or without cavitation.

In the following, we illustrate some of these developments at the *Fisica Tecnica* group of the Department of Engineering and Architecture (DIA), or in other institutions/companies in the context of collaborations and common research projects.

Pros and cons

Method	Advantages	Disadvantages
Experimental	■ More realistic	■ Need for equipment and instrumentation; ■ Problems of scale; ■ Measurement difficulties - perturbations; ■ Operating costs; ■ Times.
Analytical	■ Simple information, often in *closed* form, for general use.	■ Limited to *simple* geometry and physics; ■ Usually limited to linear problems.
CFD	■ Not restricted to linear problems; ■ *Complex* physics and geometry; ■ Stationary and non-stationary problems; ■ Costs progressively decreasing; ■ Good and/or excellent integration into the design process.	■ Discretization and modeling errors; ■ Difficulty in setting boundary conditions; ■ Simplifications; ■ Difficulties in interpretation.

CFD - and *simulation* in general - is a fundamental factor in increasing the rate of *innovation* of products and services.

Unique aspects of CFD

CFD is closer to experimental analysis than to theoretical approach, given the current limitations of the mathematical theory of partial differential equations:

- Stability;
- Error estimate;
- Convergence.

In some cases, phenomena were discovered first numerically (e.g. Campbell and Mueller 1968: subsonic ramp-induced separation [1]), and in other (rare) cases numerical simulation has disproved experimental findings affected by systematic errors (e.g. Stalio and Nobile 2003: heat transfer over riblets [2]).

In CFD, and in particular for industrial applications, it is often necessary to rely on the mathematical analysis of simplified problems, based on the assumption of linearity, but above all on heuristic reasoning, intuition, experience and *trial and error* approaches.

[1] Campbell, D. R., Mueller, T. J., A Numerical and Experimental Investigation of Incompressible Laminar-Induced Separated Flow, University of Notre Dame, Department of Aerospace Engineering, *Report UNDAS TN-1068-M1*,(1968).

[2] Stalio, E., Nobile, E., Direct numerical simulation of heat transfer over riblets, *Int. J. Heat and Fluid Flow*, **24**, pp. 356-371, (2003).

CFD *Vs* Experimental Method.

CFD techniques are not (and will not be for a long time) a complete substitute for the experimental approach:

- The (continuous) constitutive equations cannot, strictly speaking, be defined as exact;
- The discretization process - the perfect analogy between continuous and discretized equations is valid only for zero grid size - can also alter the qualitative behavior of the equations (e.g. artificial diffusivity);
- Phenomena on a very *small* scale can only be approximated (e.g. turbulence, combustion etc.).

OUTLINE

Part II

Historical notes

The beginning...

- CFD (Computational Fluid Dynamics) and CHT (Computational Heat Transfer):
  - Term *CFD* invented by C.K. Chu of Columbia University.
  - It gained popularity with P. Roache, *Computational fluid dynamics*, 1972.
- Los Alamos WWII Manhattan Project:
  - H. Bethe and R. Feynman computed the energy released for the plutonium bomb.
  - Feynman produced the first machine calculations: transition from human computers to IBM machines (done in April/May '44).
  - Bethe led the *physics* part of the calculation: two methods (1) shock capturing (unsuccessfull), (2) shock tracking (successfull).
- CFD continued to be developed at Los Alamos (hydrogen bomb):
  - Compressible flow: Richtmyer (shock capturing), P. Lax (1949-50) and F. Harlow (1952).
- These three bodies of work formed the foundation for CFD, in particular for compressible aerodynamics, that Van Leer, Jameson and Roe among others built on.
- Later on, development of CFD spread outside Los Alamos, although significant achievements continued to took place there.

(Impressive) hand calculation in 1953

Kawaguti (1953) obtained the numerical solution for the flow around a circular cylinder at a *Reynolds* number of 40, using the full N-S equations, without a computer:

- Using the $\psi - \omega$ formulation and a non-uniform mesh with 232 nodes, he was able to achieve a remarkable accurate result.
- He wrote

  The numerical integration ... took about one year and a half with twenty working hours every week, with a considerable amount of labour and endurance.

C_D value	
Kawaguti (1953)	1.618
Present (ANSYS CFX)	1.614
Lima et al., J. Comp. Physics (2003)	1.54
Anderson, Exper. (1991)	1.8

(Impressive) hand calculation in 1953 - cont.

Left: Kavaguti (1953) - 232 nodes; right: ANSYS CFX - 33500 nodes.

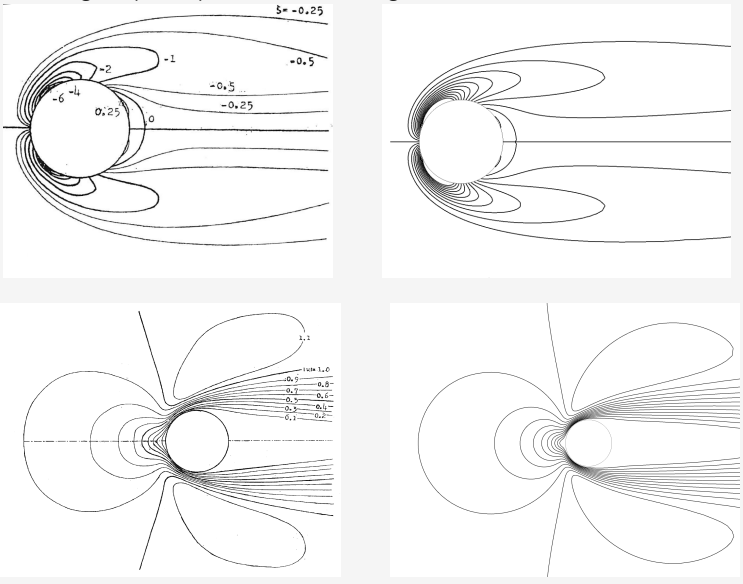

A brilliant CFD study ... *without* the computer!

Harlow and Fromm, Scientific American 1965

- *Scientific American* article of Harlow and Fromm (after *Physics of Fluids* 1965 article about *Marker and Cell* (MAC) method, later simplified in SMAC):
  - Striking, first-time visualizations of the 2D unsteady flow around a rectangular obstacle.
  - Enthusiastic - over-optimistic - view of the future of computer simulations.
  - Major impact in the scientific community.
  - Proved the capabilities of the new technology.

From left to right: mesh, streaklines and isotherms for the flow of air around a heated rectangular obstacle.

Fromm 1971

- Pioneering work of Fromm (*IBM J. Res. Develop.*, 1971) in the field of convective heat transfer.
  - Properly designed sophisticated finite difference system.
  - Performed the computation of the time-dependent, buoyant chaotic flow in a square cavity at values of the *Rayleigh* number as high as 10^{12}.
  - Several years before similar simulations were attempted by Paolucci, Le Quéré and Nobile.

From left to right: instantaneous streamlines, vorticity and isotherms for the buoyant flow in a square box at a *Ra* number of 10^8.

Programming languages

At the beginning, major part of code development was done *in-house*:

- Each research group had their own code(s), most of the times written in *FORTRAN IV*.
- Difficulties in implementing new models and algorithms.
- Programming done by experts in the specific thermal-fluid domain.
- Minor attention to readability, maintainability, proper documentation et.
- Corresponding codes were hard to read and interpret for those who did not write it - and even for those who wrote it after some time - with waste of time and resources.

Programming languages - cont.

Comparison of a piece of a FORTRAN code, modified by the present author in 1987, with a snippet of modern *Julia* code.

```
      PROGRAM COLL       73/172  OPT=0,ROUND= A/ S/ M/-D,-DS     FTN 5.1+6
455               A(7*(MAXR/2)-6,5)=-XMAXR
456               A(7*(MAXR/2)-6,8)=XMAXR**2/(XMAXR-1.0)
457               A(3,6)=XMAXR
458               A(7*(MAXR/2-1)-1,8)=-DIVZ
459               A(7*(MAXR/2)-5,8)=-DIVZ
460               A(7*(MAXR/2)-3,3)=HALFM
461               A(7*(MAXR/2)-3,8)=-HALFM
462               A(1,9)=HALFM*3.0
463               A(1,13)=-HALFM*4.0
464               A(1,16)=HALFM
465               G1=COL/GNUM8R
466               G2=-G1*C03
467               C08=C03+1.0
468               TCOMMN=G1*T(2,2)+C02
469               TALPHA=TCOMMN**(-C03)
470               TBETA=G2*TCOMMN**(-C08)
471               TONE=TBETA*(T(2,3)-T(2,2))
472               TTWO=TBETA*(T(2,2)-T(1,2))*DIZS9
473               VONE=HALFM*V(2,2)
474               TFOUR=TALPHA*3.0
475               TSIX=TALPHA*DIZS9
476               A(2,13)=VONE*(TFOUR+0.5*TONE)-VONE
477               UONE=DIVZ*U(2,2)
478               A(2,9)=UONE*(TALPHA-0.5*TONE)+VONE+DIVRE*(TALPHA*MTWO+2.
479              1-UONE
480               A(1,12)=VONE*(TFOUR+TONE)-VONE
481               VARIT=TALPHA*(DIZS9-SQN2*6.0)
482               A(1,8)=UONE*(TALPHA-TONE)+VONE+DIVRE*(VARIT+TTWO)-UONE
483               SONE=V(2,2)*(-U(2,2)*DIVZ+DIVRE*(2.0*TSIX+TTWO))
484               STWO=-DIVRE*(V(1,2)*TSIX+HALFM*DELTZ*TTWO*(U(2,3)-U(2,2
485               B(1)=SONE+STWO
486               UPGRDN2=UP1+T(2,2)*(UP2+UP3*T(2,2))
487               BONE=UPGRDN2-DIVZ*(P(2,2)+U(2,2)**2)-U(1,2)*TALPHA*DIVR
488               BTWO=DIVRE2*U(2,2)*(TSIX+TTWO)-DIVRE4*TONE*(V(2,2)-V(1,
489               B(2)=BONE+BTWO
490               TCOMMN=G1*T(2,MAXR)+C02
491               TALPHA=TCOMMN**(-C03)
492               TBETA=G2*TCOMMN**(-C08)
493               IF(ITALLY.EQ.0) GO TO 114
494               TONE=TBETA*(T(2,MAXR)+HFLUXM-T(2,MAX1))
495               GO TO 113
496           114 TONE=0.0
497           113 CONTINUE
```

```
using LinearAlgebra
using Random

function domeigen(A, p)
    b₀ = similar(A, size(A, 1))
    rand!(b₀)

    # power iteration
    bₖ = b₀
    for _ in 1:p
        bₖ₊₁ = A * bₖ

        # normalize
        bₖ = bₖ₊₁ / norm(bₖ₊₁)
    end

    # Rayleigh quotient
    λ = (A*bₖ ⋅ bₖ) / (bₖ ⋅ bₖ)

    return bₖ, λ
end
```

Real Programmers use FORTRAN!

Software development

Size of OpenFOAM and modeFRONTIER (2018R2):

Metric	modeFRONTIER	OpenFOAM
Lines of code	1.085.133	$\approx$ 1.000.000
Number of classes	12.668	-
Unit tests	23.586	-
Test coverage	36.1 %	-

Software Maintenance & Evolution:

- ➢ Big challenge for medium/small organizations.
- ➢ Highly expensive for bad quality software.

From structured to unstructured grids

- First general purposes codes based on single-block structured hexahedral grids:
  - (+) Efficient data structure and memory usage.
  - (-) Limited geometrical flexibility.
  - (-) Unsuitable to handling the complex geometries required for industrial applications.
- Finite Element Method (FEM), largely employed in structural analysis, had already the capability to handle arbitrary geometries through unstructured grids.
- Major effort towards development of unstructured grids for the Finite Volume Method (FVM).
- This culminated in the widely used cell-centered, collocated unstructured FVM with cells of arbitrary topology (Demirdžič and Muzaferija, 1995).
- Approach adopted in most commercial and open source CFD packages, but it has disadvantages:
  - possible inaccuracies in the *reconstruction of the gradient*.
  - inefficient treatment of the diffusion term for complex, highly distorted grids.

An efficient cell-centered unstructured grid approach

B. Niceno (PSI) developed and tested a staggered, unstructured FVM for cells of arbitrary topology (ECCOMAS 2006):

- More demanding in terms of memory requirement and slightly more expensive, it has several favorable features:
  - No need of any stabilization procedure (Rhie & Chow, Arakawa, addition of 4^{th} Order dissipative terms et.) to couple velocity and pressure.
  - No need of *deferred correction*.
  - It is *(turbulence) energy conservative* (LES).

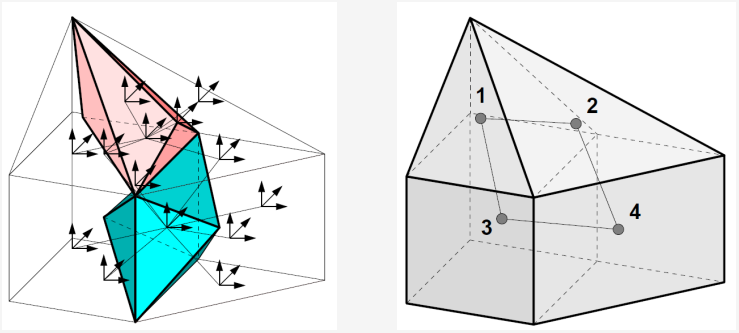

Finite Volumes for (left) momentum equation and (right) pressure equation.

Vector processors

- From the beginning of CFD, it was evident that its computational requirements was very high:
  - Intrinsic non-linearity of the governing equations.
  - Necessity to resolve boundary layers, regions with high gradients et.
- Mainframes available in the 1970s struggled to perform CFD calculations.
- Effort to develop faster computing platforms, which gave rise to the *vector processors*, e.g. CPUs that operate on 1D arrays of data.
- Cray family of vector supercomputers: Cray-1, Cray-XMP, Cray-YMP and Cray-2.
- Other companies: Control Data Corporation (Cyber 205), Fujitsu, Hitachi, Nippon Electric Corporation (NEC) et.,
- All, but NEC, abandoned the market and invested more on massively parallel machines.
- Experience in programming the IBM 3090 VF (Vector Facility) and Cray family (Cray-XMP and Cray-YMP):
  - Attainment of good performances with the IBM 3090 VF not an easy task.
  - Good performances on the Cray machines (time-dependent and chaotic flows).

Fortran coding on the CRAY X-MP, 1993

```
      subroutine add_correct(k_grid, vx, vy, prs, temp,
     .                       icvx, icvy, loff)
* I-------------------------------------------------------I
* I          C R A Y     V E R S I O N                    I
* I                                                       I
* I    1. UNROLLING OF A SHORT LOOP                       I
* I    2. FORCED VECTORISATION OF INNERMOST LOOP          I
* I-------------------------------------------------------I
*  Add corrections from the coarser to the actual grid....
*
      dimension vx(*), vy(*), prs(*), temp(*)
      dimension icvx(*), icvy(*), loff(*)
*
      do ikp1 = 2, icvy(k_grid+1)+1
CDIR$ IVDEP$
      do jkp1 = 2, icvx(k_grid+1)+1

         lockp1  = loff(k_grid+1)+(icvx(k_grid+1)+2)*
     +             (ikp1-1)+jkp1
         ik      = 2*ikp1-2
         jk      = 2*jkp1-2
         lock1   = loff(k_grid)+(icvx(k_grid)+2)*
     +             (ik-1)+jk
         lock2   = lock1+1
         lock3   = lock1+icvx(k_grid)+2
         lock4   = lock3+1
*
         vx(lock1)   = vx(lock1)  +  vx(lockp1)
         vx(lock2)   = vx(lock2)  +  vx(lockp1)
         vx(lock3)   = vx(lock3)  +  vx(lockp1)
         vx(lock4)   = vx(lock4)  +  vx(lockp1)
*        [.....]
      end do
      end do
*
      return
      end
```

Vectorized coupled solvers

- E. Nobile, Simulation of Time-dependent Flow in Cavities with the Additive Correction Multigrid Method, Part I: Mathematical Formulation, *Numerical Heat Transfer, Part B: Fundamentals*, **30**, No. 3, pp. 341-350, (1996).
- E. Nobile, Simulation of Time-dependent Flow in Cavities with the Additive Correction Multigrid Method, Part II: Applications, *Numerical Heat Transfer, Part B: Fundamentals*, **30**, No. 3, pp. 351-370, (1996).

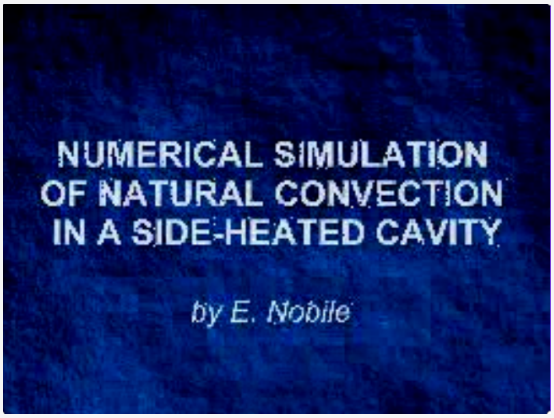

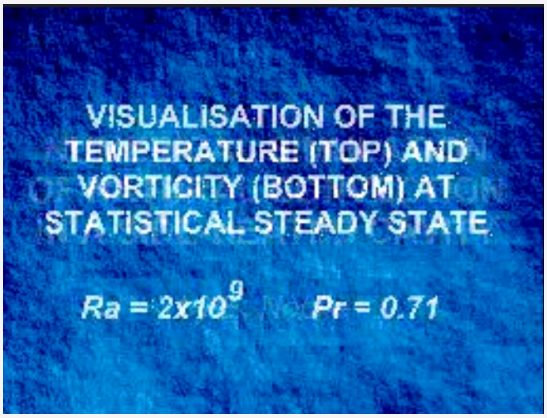

GPU

- Interest in vector processing revamped due to widespread availability of Graphic Processing Unit (GPU) and their increasing performances.
- GPUs include an array of shader pipelines which can be considered vector processors.
- Most HPC (High Performance Computing) manufacturers provide, among their offer, hybrid machines, e.g. CPUs+GPUs systems.
- Several CFD software vendors can - at least partially - exploit the GPUs if available.

Multiphase heat transfer

- Multiphase heat transfer: boiling, condensation, solidification et.
- Modeling of these phenomena is challenging!
- High-fidelity simulation - by e.g. DNS (Direct Numerical Simulation), LES (Large Eddy Simulation) or DES (Detached Eddy Simulation) - nowadays routinely performed for single-phase problems.
- *First principle* approach difficult, if not impossible, for many multiphase problems of scientific and practical interest.
- Reference book on direct numerical simulations of gas-liquid multiphase flows:

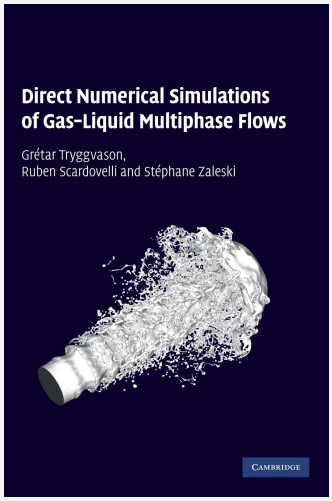

The beginning

- In 1969 B.D. Spalding, professor of Heat Transfer at Imperial College (IC), UK, founded the company *CHAM* (Combustion, Heat And Mass Transfer, Ltd., later superseded by Concentration, Heat And Mass Transfer, Ltd.).
- Gosman et al., *Heat and Mass Transfer in Recirculating Flows*, 1969.
- *PHOENICS* (Parabolic Hyperbolic Or Elliptic Numerical Integration Code Series) code from CHAM launched in 1978.
- *FLUENT* started in 1983 at Creare Inc. (Etna, NH, USA), by J. Swithinbank and F. Boysan at Sheffield University, UK:
  - Fluent Inc. founded in 1988, Lebanon, NH, USA.
  - In 1995, Fluent Inc. acquired by heat sink producer Aavid Thermal Technologies.
  - In 1996, Fluent Inc. acquired Fluid Dynamics International (FDI), Evanston, IL, which developed *FIDAP* (co-founded by M. Engelman and S. Rosenblat in 1982).
  - In 1997 acquired Polyflow S.A., a Belgian company developer of POLYFLOW.
  - Aavid acquired by Chicago private equity firm Willis Stein and Partners (WSP) in 1999 for US$ 260 million.

New players

- In the middle of 1980s, D. Gosman and R. Issa formed Computational Dynamics (CD) Ltd.:
  - Adapco backed CD to produce a body-fitted CFD code named *STAR-CD* (*Simulating Transport in Arbitrary Regions*).
  - First version block-structured but second release in 1991 unstructured (first unstructured commercial code).
  - *STAR-CCM+* launched after a development phase commenced in 1999.
  - *CD-Adapco* acquired by Siemens in 2016 for $970 million.
- UK's Atomic Energy Authority (AEA) privatized a portion of itself in 1996 as *AEA* Technology, which contained their CFD business, *Harwell-FLOW3D*, later renamed to *CFX*:
  - Up to Rel. 2 of Harwell-FLOW3D limited to curvilinear, single-block structured grids.
  - In 1993, with Rel. 3.2, it added multi-block capability.
  - Development of their unstructured code (*ASTEC*) abandoned after acquisition of *TASCflow* from Advanced Scientific Computing (ASC) of Waterloo, Ontario, CDN.
- ANSYS, renowned for its structural analysis tools:
  - In 2003 acquired the of CFX division of AEA technology (ICEM CFD was acquired in 2000).
  - Purchased *Fluent* from WSP in 2006 for US$ 630 million.
  - Had to obtain FTC (Federal Trade Commission) clearance for the Fluent acquisition.

Other players, M&A

A *not-exhaustive* list:

- Flow Science Inc. (FLOW-3D)
- Numeca (Fine, Omnis)
- ESI (ACE+, ESI-PRESTO, Systus, Visual-CFD for OpenFOAM)
- Convergent Science (CONVERGE CFD)
- Siemens (STAR-CCM+)
- Autodesk (Autodesk ® CFD)
- Dassault Systèmes (Abaqus/CFD, XFlow, SCStream, PowerFLOW® CFD
- SOLIDWORKS® Flow Simulation, Simerics MP for SOLIDWORKS)
- MSC (scFLOW, scSTREAM, sc/Tetra)
- AVL (AVL FIRE™).

Web browser based simulation (es. SimScale).

Harwell-FLOW3D-Rel. 2

- Purchased (tapes...) in 1990.
- Deployed at the University of Trieste Central Computing Center (Centro di Calcolo):
  - Grid generator, Pre- and Post-processor on a Digital VAX VMS 780.
  - Solver on a CRAY X-MP/14se: theoretical peak performance of 200 Mflops.
  - Iphone 7 Plus (12 Pro Max), Multithreaded mode enabled/disabled, LINPACK 1000 $\times$ 1000: *6570/3450 (10589/5035* Mflops.

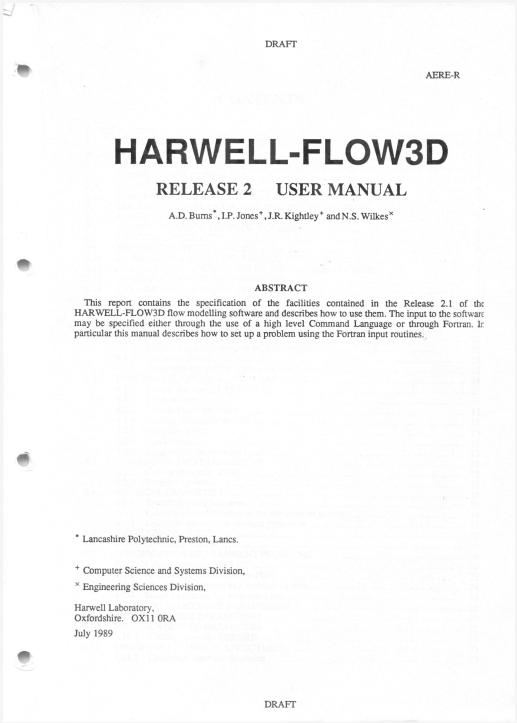

DRAFT

AERE-R

HARWELL-FLOW3D

RELEASE 2 USER MANUAL

A.D. Burns*, I.P. Jones*, J.R. Kightley* and N.S. Wilkes×

ABSTRACT

This report contains the specification of the facilities contained in the Release 2.1 of the HARWELL-FLOW3D flow modelling software and describes how to use them. The input to the software may be specified either through the use of a high level Command Language or through Fortran. In particular this manual describes how to set up a problem using the Fortran input routines.

* Lancashire Polytechnic, Preston, Lancs.

+ Computer Science and Systems Division,
× Engineering Sciences Division,

Harwell Laboratory,
Oxfordshire. OX11 0RA

July 1989

DRAFT

Iridotomy, 1991

- Evaluation of the effect of iridotomy's diameter in the reduction of pressure difference between anterior and posterior chambers of the eye for patients suffering from acute glaucoma.
- Among one of the first CFD applications in this particular field.

- Computational domain, axial-symmetric grid and detail of the velocity field for an iridotomy diameter of 100 μm:

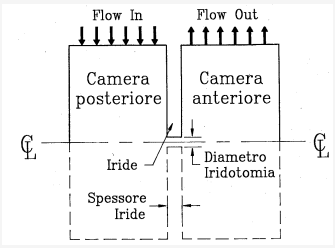

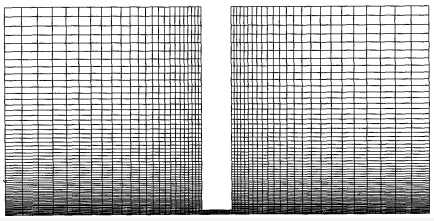

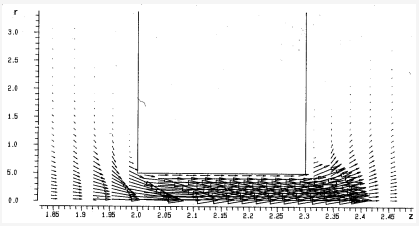

CFD Open Source

Usually provided under a software license that permits users to study, change, and improve the software.

- Most widely used open-source CFD software package is *OpenFOAM*:
  - Official *OpenFOAM* release maintained by the *OpenFOAM Foundation*.
  - Some companies have developed code variations to commercialize their additions to the code.
- *SU2*, developed mainly at Stanford University and particularly oriented towards external aerodynamics.
- *Basilisk*, successor of the *Gerris* flow solver:
  - Strong capabilities in modelling multiphase, free surface flows.
  - Use of quad-tree (in 2D) and oct-tree (in 3D) adaptive grids.
- *Palabos* CFD solver:
  - Based on the Lattice-Boltzmann Method (LBM).
  - New product OMNIS™/LB from Numeca integrated *Palabos* in a monolithic enhanced configuration, with a large range of functionalities.

NASA CFD Vision 2030

NASA/CR-2014-218178 - CFD Vision 2030 Study: A Path to Revolutionary Computational Aerosciences

- Provides a *knowledge-based forecast of the future computational capabilities required for turbulent, transitional, and reacting flow simulations...*.
- Not strictly related to CHT, but might be of interest to the thermo-fluid community.
- Some of the topics of the NASA document are addressed in the following, together with others which might be of specific interest to CHT.

Multiobjective and robust optimization

- Use of *optimization* methods has gained more acceptance within the Heat Transfer community, with applications ranging from component to system level.
- Presence of uncertain model data, e.g. initial and boundary conditions, thermo-physical properties of the medium and uncertainties (tolerances) in geometrical dimensions:
  - Need for efficient uncertainty quantification (UQ) for establishment of confidence intervals in computed predictions.
  - Optimization under uncertainty, e.g. *robust* optimization.

Shape optimization of a tube bundle in cross-flow

- Ranut et al., *Multi-objective shape optimization of a tube bundle in cross-flow*, 2014:
  - Three simultaneous - and conflicting - objectives considered, e.g. Maximization of the heat transfer rate outside the tubes, minimization of the pressure loss for the external flow and minimization of the pressure loss for the internal flow.
  - Sketch of the problem, tube shape parametrization and domain used for the periodic simulation at the shell side:

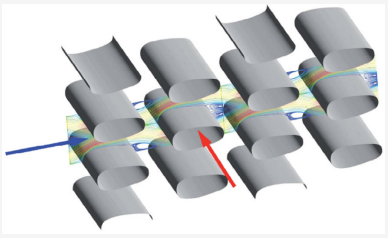

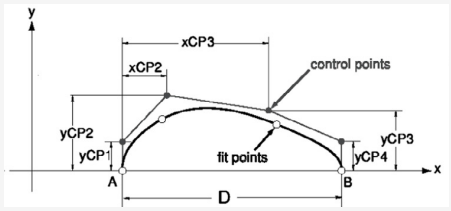

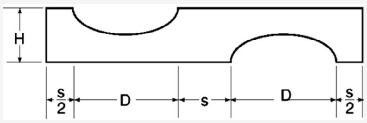

Shape optimization of a tube bundle in cross-flow - cont.

2D visualizations of the objective space Δp_{tube} - ΔP_{shell} and ΔT_{per} - Δp_{shell} together with some of the optimal designs and visualizations of flow and temperature fields for design number 894.

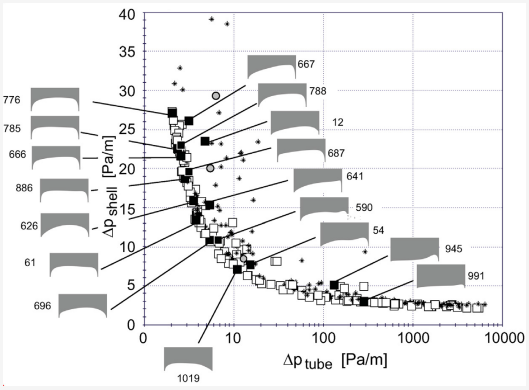

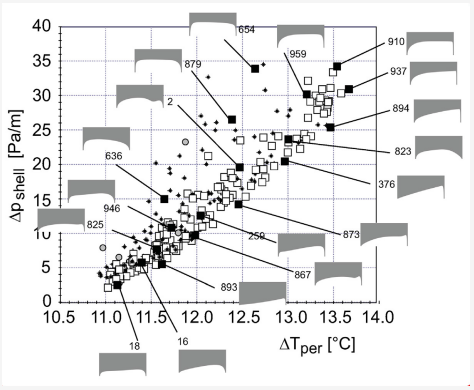

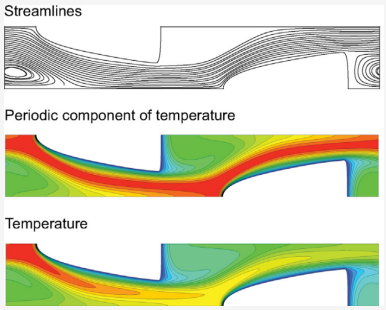

Low vs High order methods

- Many industrial - commercial or open source - CFD and CHT tools based on cell-centered or node-(vertex) centered FVM:
  - Limited in most cases to 2^{nd} order discretization of the underlying conservation equation.
  - Practical applications frequently require tens or even hundreds of million mesh points.
- Increasing interest in *Scale resolving simulations*, like *LES* (Large Eddy Simulations) and *DES* (Detached Eddy Simulations), for practical problems:
  - Can require very fine meshes and thousands of small time steps to resolve the energy containing part of the turbulence spectrum and to achieve significant statistical results.
- Use of *high order* methods - order greater or equal to three - would be extremely beneficial, since the reduction in the number of grid points would more than compensate the increase of the computational cost.
- High-order methods are in general less robust and more prone to instabilities and convergence difficulties.
- Major effort in the development of high-order CFD methods, e.g. EU funded project *IDIHOM* (Industrialisation of high-order methods).
- Review of high order methods by Huynh et al., 2014:
  - Proposed Flux Reconstruction (FR) approach or Correction Procedure using Reconstruction (CPR).
  - Unifies the most important high-order methods, i.e. Discontinuous Galerkin (DG), Spectral Difference (SD) and Spectral Volume (SV) methods.

Multiscale simulations

- Several heat transfer and fluid flow problems are *multiscale*:
  - Thermal control in a data center.
  - Fuel cells.
- *Multiscale numerical methods* are needed.
- Include macroscopic standard continuum methods, e.g. Navier-Stokes and energy equations; mesoscopic particle-based lattice Boltzmann, direct simulation Monte Carlo, dissipative particle dynamics and microscopic molecular dynamics.
- Recent (2019) review of Tong et al. provides an extensive review of current progresses of the multiscale simulations for fluid flow and heat transfer problems.

Do we need a mesh ?

- In traditional methods, like i.e. FVM and FEM, nodes (or cell centroids) are connected to a certain number of neighbors through a *mesh* or *grid*:
  - For cell-centered FVM, the grid defines the geometric properties of each cell and the *connectivity* between the centroids.
  - Connectivity required to construct mathematical operators, e.g. the *gradient*.
- The mesh must possess certain requisites, i.e. degree of orthogonality, minimum skewness et., to guarantee accurate and stable simulations.
- In some situations these requisites are hard to maintain and lead to either increase of computational costs or catastrophic failures.

Why meshless

- *Meshless* or *Meshfree* methods: avoid any mesh at all, and compute directly the interaction of each node with some of its neighbors which are typically within a given distance.
- *Meshless* methods enable the computation of some otherwise difficult problems, at the cost of some extra computing time and programming effort (till now).
- Absence of a mesh allows *Lagrangian simulations*, in which the nodes can move according to the velocity field.

Meshless methods

Several *meshless* methods for CFD and CHT applications:

- *SPH* - Smooth particle hydrodynamics.
- *MPS* - Moving particle semi-implicit.
- *PIC* - Particle-in-cell.
- *MLS* - Moving least squares.
- *LRBFCM* - Local radial basis function collocation method, also known as radial basis function generated finite differences (*RBF-FD*) method.

Example of use of *MPS*

Use of *MPS* (Particleworks) methos for the simulation of cooling of a medium speed engine piston (courtesy of S. Ojala):

- Instantaneous position of fluid particles and computed time-averaged heat transfer coefficient.
- Fluid particles represent the oil jet used to cool the piston.
- Free surface and surface tension.

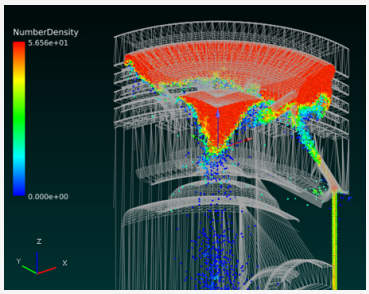

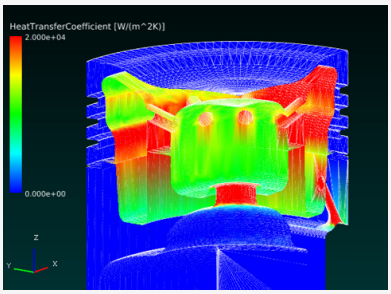

Simulation time comparison:

Parameter	MPS (Particleworks)	VOF
Physical time (one piston stroke) [s]	0.1	0.1
Part. diam. (MPS)/avg. cell size (VOF) [mm]	1.75	2
N. CPU/GPU cores	2 CPUs / 1 GPU	160 CPUs
Simulation time [h]	5	24

LRBFCM @UniTS

- Development of LRBFCM at University of Trieste (R. Zamolo, B. Šarler):
  - Techniques to place the nodes in a very general and flexible way.
  - Increase the computational performances of the method.
- Images approximated through the *stippling* technique:

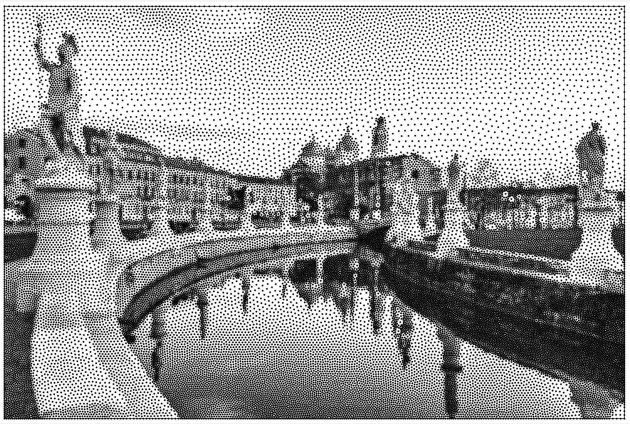

LRBFCM @UniTS - *cont.*

UIT Heat Transfer Conference 2019

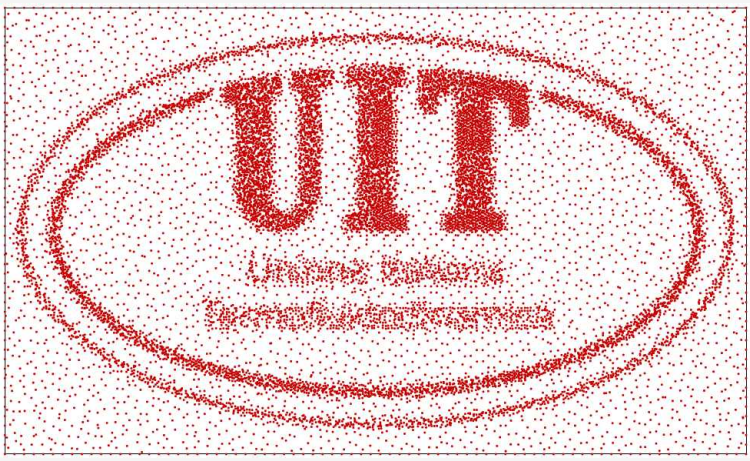

LRBFCM @UniTS: examples

Backward facing step

- Computational domain

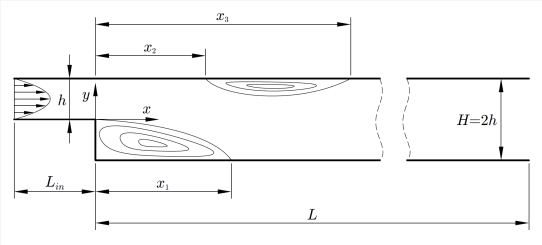

- Details of nodes distribution

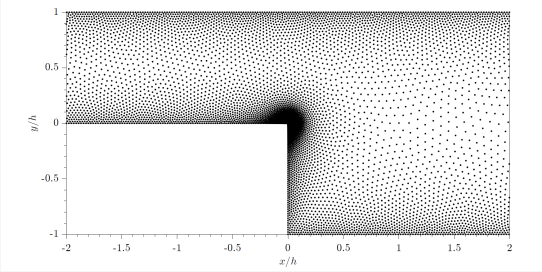

Microchannel

- Computational domain

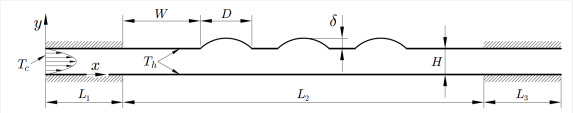

- Details of nodes distribution

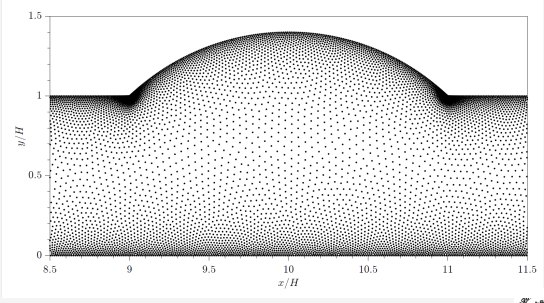

LRBFCM @UniTS: examples- *cont.*

Flow around a cylinder at $Re = 2000$ and buoyant flow in a square cavity at $Ra = 4 \times 10^8$:

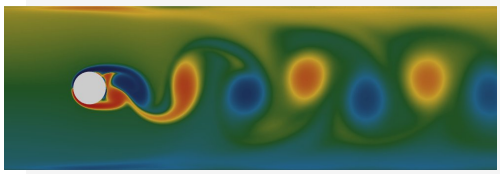

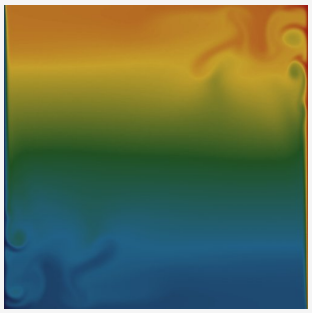

Machine Learning and AI

- *Machine learning* (ML): algorithms and statistical models that computers use in order to perform a specific task without using *explicit instructions*, but rather relying on *patterns*.
- ML algorithms build a mathematical model based on sample data (*training data*) in order to make predictions without being explicitly coded to perform the task.
- ML and *optimization*: minimization of some loss function on a training set of examples.
- Growing interest of ML models in thermal fluid simulation:
  - Advent of data-intensive thermo-fluid experiments and high-fidelity numerical simulations.
  - Affordable computing platforms.
  - Progress in ML methods: deep learning using multilayer neural networks (NN).
- With reference to CFD and CHT, ML can be defined as the capability to create effective *surrogates* from a massive amount of data (measurements and/or simulations).
- Concept of *physics-informed neural networks*.

ML example: boiling

Liu et al. (ATE, 2018) used a deep feedforward neural network (DFNN) to predict boiling heat transfer:

- ➢ Inputs: local momentum and energy convective transport, pressure gradients, turbulent viscosity, surface information.
- ➢ Outputs: quantities of interest (heat transfer components, wall superheat, near wall void fraction).
- ➢ Networks trained by high-fidelity data from first principle simulation of pool boiling.

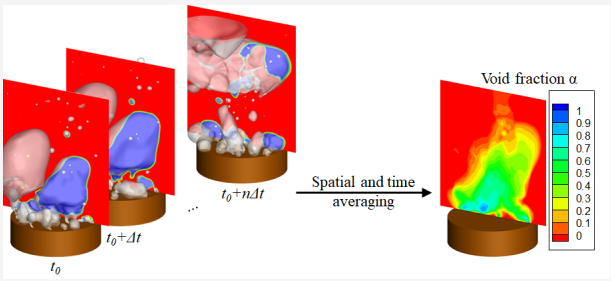

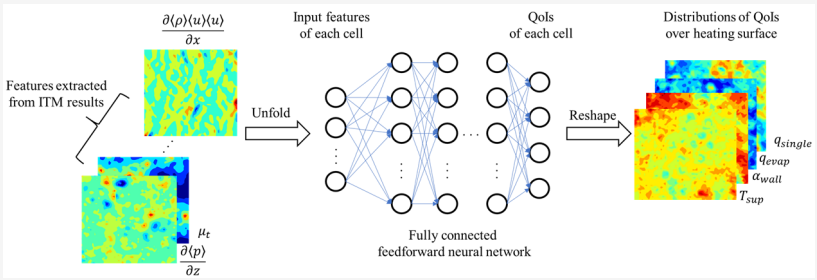

ML example: boiling - cont.

Predictive capability of the DFNN by comparison between DFNN predictions and the original ITM (Interface Tracking Method) results on the heating surface:

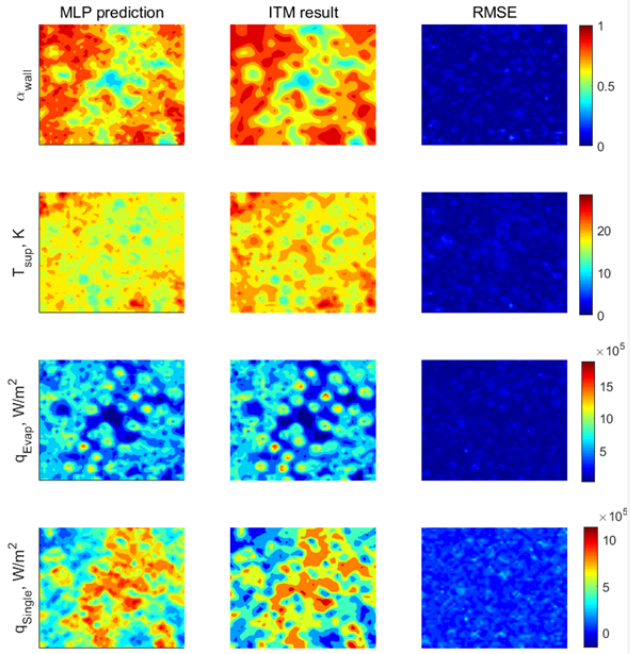

The DFNN prediction captures both the local boiling process and the global boiling pattern with good accuracy.

What's next ?

- Some milestones in the history of CFD (review *biased* by personal experience).
- From an esoteric discipline to an advanced technology for the aeronautical and nuclear sector, CFD and CHT eventually went mainstream, with pervasive applications in almost any field.
- Different level of maturity of CFD and CHT.
- Fundamental and applied research required to advance the credibility level in e.g. turbulence, multiphase flows, et.
- While noteworthy progress has been obtained, in some cases the experimental methods still represent the most reliable tools.
- Dramatic increase of performance of computing hardware in recent years.
- Lag of software: legacy codes, which in some cases date back to the 80's, are still the workhorse in several research applications.
- New and exciting opportunities for research:
  - ➢ Relentless increase of performance of novel dedicated hardware.
  - ➢ Development of new numerical algorithms.
  - ➢ New programming paradigms.
  - ➢ Machine learning and AI technologies.
  - ➢ Quantum computing.

What's next ? Is *Quantum Computing* the next revolution for CFD??

It seems that, from many sources, *Quantum Computing* (QC) is the key-enabler for (almost) real-time, ultra-high resolution (DNS) for CFD. Is this true?

- *... It is clear that the era of QC is here ... the CFD community, along with other aeroscience and engineering communities, needs to recognize this evolution and understand that this is not a short-term endeavor.* [*AIAA JOURNAL* Vol. 58, No. 8, August 2020 - Quantum Speedup for Aeroscience and Engineering, P. Givi, A.J. Daley, D. Mavriplis, M. Malik].
- *... Finally, let us consider the IBMQ 54-qubit machine for some specific remarks.*
  ... 2. DNS grid sizes: With a 54-qubit machine we can store and compute on
  1. 1D: $\leq 10^{16}$ meshes
  2. 2D: $\leq 10^8 \times 10^8$ meshes
  3. 3D: $\leq 10^5 \times 10^5 \times 10^5$ meshes

  Here, each of these mesh sizes is far higher than the largest available DNS computations at present. [*Indian Academy of Sciences Conference Series* (2020) 3:1 - Quantum computation of fluid dynamics, S.S. Bharadwaj, and K.R. Sreenivasan].

But...

- *... In actual practice, QC ensemble simulations of the Navier?Stokes equations demand hundreds of noiseless logical qubits. Given that current quantum computing typically works only up to a few logical qubits, say of the order ten, the target appears pretty much into the future.* [*Computers and Fluids* 270 (2024) 106148 - S. Succi, W- Itani, C. Sanavio, K.R. Sreenivasan, R. Steijl]

Latest new in *Quantum Computing*

In February 19, 2025, Microsoft announced their new *Majorana 1 chip*:

- *... Microsoft today introduced Majorana 1, the world's first quantum chip powered by a new Topological Core architecture ...*
  - *...It leverages the world's first topoconductor, a breakthrough type of material which can observe and control Majorana particles to produce more reliable and scalable qubits, which are the building blocks for quantum computers.*
  - *...In the same way that the invention of semiconductors made today's smartphones, computers and electronics possible [...] to developing quantum systems that can scale to a million qubits and are capable of tackling the most complex industrial and societal problems, Microsoft said.*

But...

- Microsoft's quantum hardware has been the subject of *controversy* since its high-profile *retracted article from Nature in 2018*, and the announcement of Majorana 1 has generated both excitement and skepticism within the scientific community.

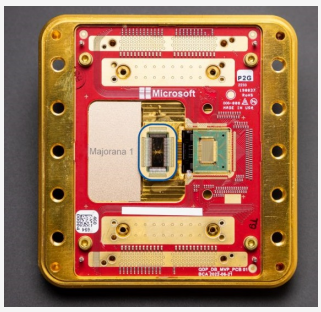

OUTLINE

Part III

Applications

Cavitation

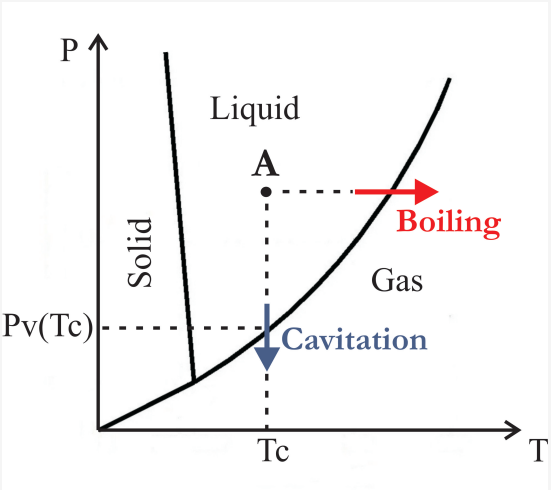

Cavitation can be defined as:

- The vaporization of a liquid when the (static) pressure drops to values lower than those of the corresponding saturation pressure [1]
- The formation and activity of bubbles - or cavities - in a liquid [2]
- The *collapse* (breakdown) of a liquid under very low pressure conditions [3]

[1] Coutier-Delgosha, O., Reboud, J., Delannoy, Y., Numerical simulation of unsteady behaviour of cavitating flows, *Int. J. Num. Meth. Fluids*, **42**, pp. 527-548, (2003).

[2] Young, F., *Cavitation*, Imperial College Press, London, (1989).

[3] Franc, J., Michel, J., *Fundamentals of Cavitation*, Kluwer Academic Publisher, (2004).

Examples of hydrodynamic cavitation

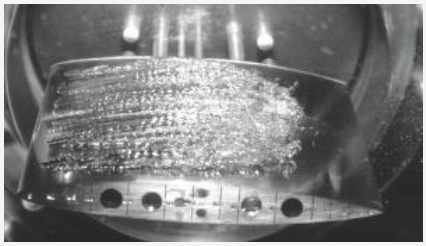
Partial Cavitation

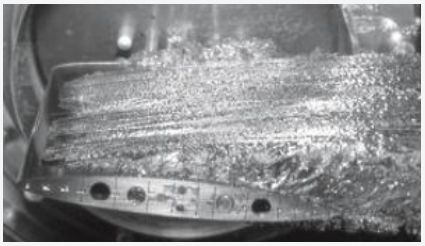
Supercavitation

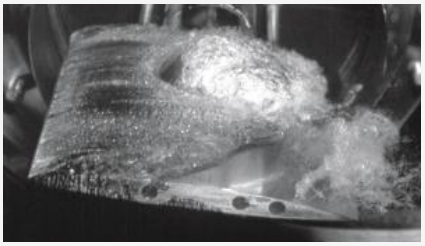
Cloud Cavitation

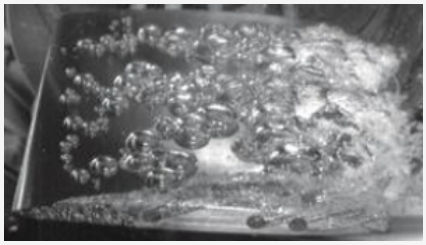
Bubble Cavitation

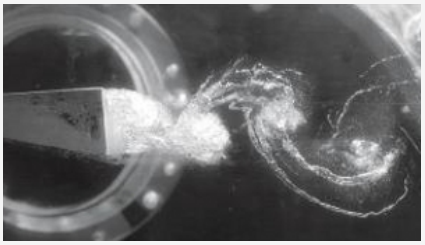
Vortex Cavitation

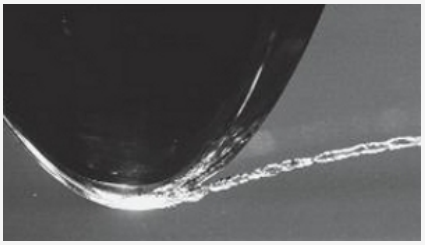
(Tip) Vortex Cavitation

Figures taken from: *Fluid Dynamics of Cavitation and Cavitating Turbopumps*. Edited by D'Agostino, L., and Salvetti, M.V., 2007

Propeller E779A

- Test cases for *validation* of CFD codes/procedures;
- Property of CNR-INSEAN (The Italian Ship Model Basin) `http://www.insean.it/`;
- Diameter D = 0.2272 m

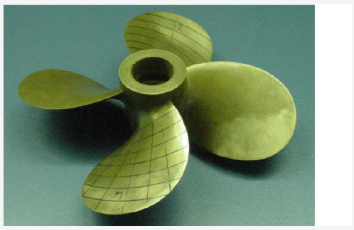
Propeller E779A

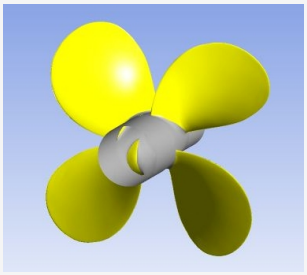
Propeller E779A: CAD model

- Steady-state simulations;
- MRF (Multiple Reference Frame) approach;
- Domain divided into two parts:
  - *Rotating*
  - *Fixed*

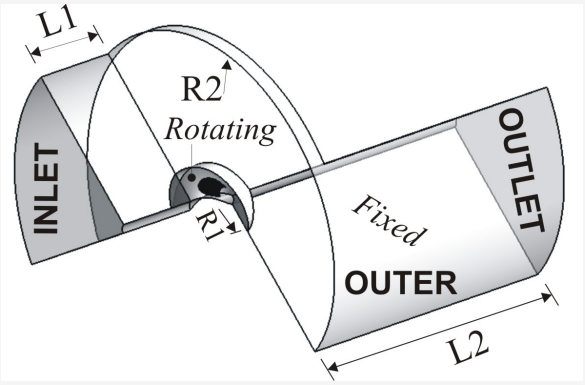

Computational domain

Propeller E779A - Cavitation Patterns

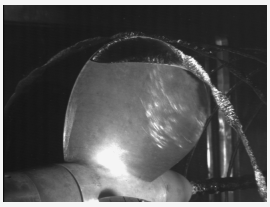

Exp. J=0.71, $\sigma_n = 1.763$

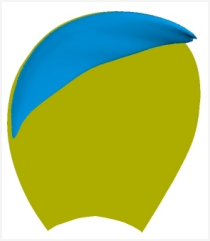

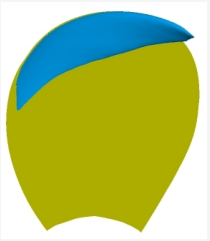

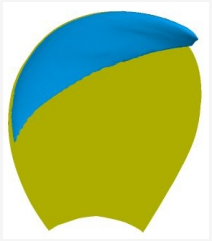

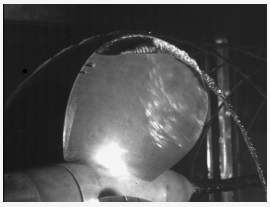

Exp. J=0.77, $\sigma_n = 1.783$

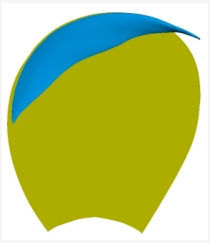

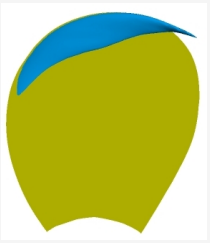

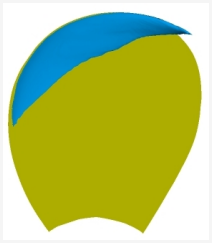

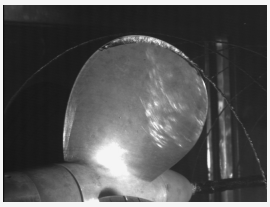

Exp. J=0.83, $\sigma_n = 2.063$

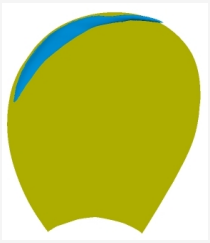

Zwart

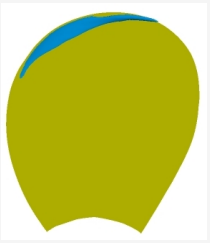

FCM

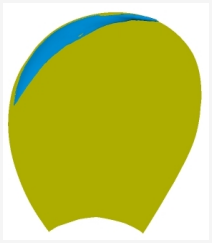

Kunz

$$J = \frac{V}{nD} \qquad \sigma_n = \frac{P_{ref} - P_v}{0.5\rho_l (nD)^2}$$

Propeller E779A - thrust and torque

Numerical results at J=0.71 for $\sigma_n = 1.763$
and for the non cavitating regime

	Non-Cavitating		Cavitating	
	Kt	Kq	Kt	Kq
Measured	0.256	0.464	0.255	0.46
SST	0.246	0.442		
Zwart+SST			0.252	0.453
FCM+SST			0.249	0.446
Kunz+SST			0.253	0.453
RSM	0.247	0.441		
Zwart+RSM			0.252	0.450
FCM+RSM			0.249	0.443
Kunz+RSM			0.253	0.451

$$J = \frac{V}{nD} \qquad \sigma_n = \frac{P_{ref} - P_v}{0.5\rho_l (nD)^2}$$

$$Kt = \frac{T}{\rho_l n^2 D^4} \qquad Kq = \frac{Q}{\rho_l n^2 D^5}$$

SST = Shear Stress Transport

RSM = Baseline Reynolds Stress Model

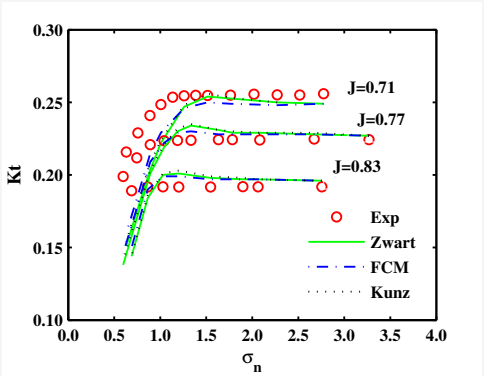

Influence of the cavitation number σ_n and of the mass transfer model on the thrust coefficient.

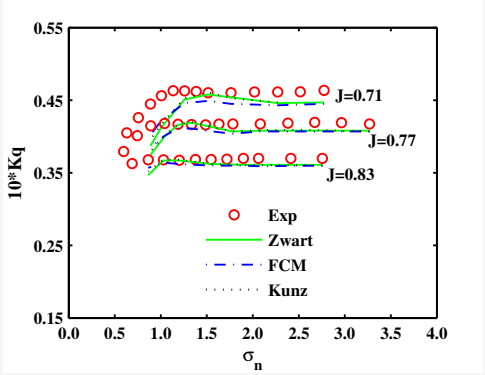

Influence of the cavitation number σ_n and of the mass transfer model on the torque coefficient

SMP11 - Workshop Propeller performance

Second International Symposium on Marine Propulsors 2011
Workshop: Propeller performance
17 - 18 June 2011, Hamburg, Germany

- Potsdam Propeller Test Case (PPTC)
- Cavitation Tests with the Model Propeller VP1304
- Case 2.3
- Blind Benchmark
- Proceedings available on-line:
  http://www.marinepropulsors.com/smp/files/downloads/smp11_workshop/smp11_workshop/

SMP11 - Workshop Propeller performance

Eleven participating groups

Group	Solver	Acronym
Berg-Propulsion	Procal	Berg-Procal
Cradle	SC/Tetra	Cradle-SC/Tetra
CSSRC	ANSYS Fluent	CSSRC-Fluent
HSVA	QCM	HSVA-QCM
	PPB	HSVA-PPB
INSEAN	PFC	INSEAN-PFC
SSPA	ANSYS Fluent	SSPA-Fluent
TUHH	FreSCO+	TUHH-FreSCO
University of Genua	Panel	UniGenua-Panel
	StarCCM+	UniGenua-StarCCM
University of Triest	ANSYS CFX(FCM)	UniTriest-CFX(FCM)
	ANSYS CFX(Kunz)	UniTriest-CFX(Kunz)
	ANSYS CFX(Zwart)	UniTriest-CFX(Zwart)
VOITH	Comet	VOITH-Comet
VTT	FinFlo	VTT-FinFlo

SMP11 - Propeller PPTC

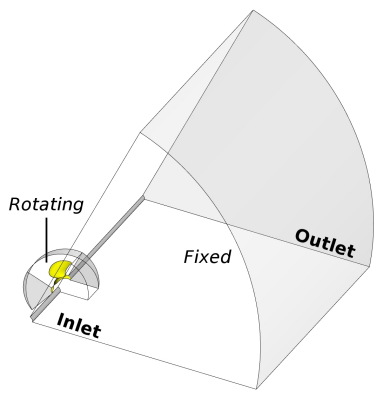

Computational Domain

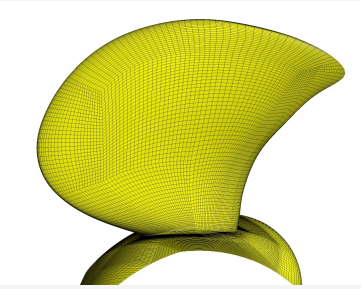

Blade surface mesh

- Steady state simulations
- MRF approach
- SST turbulence model
- Domain split in two parts
  - Rotating Part: *Rotating*
  - Stationary Part: *Fixed*
- *Rotating* = 1838655 nodes
- *Fixed* = 275680 nodes

SMP11 - Cavitation patterns

Experiment

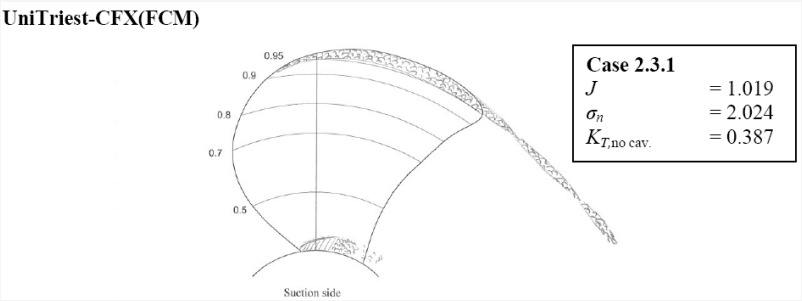

Calculation

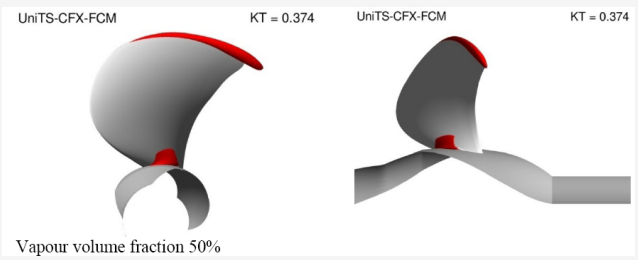

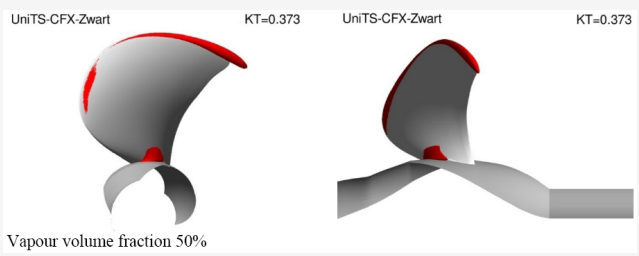

SMP11 - Cavitation patterns

Experiment

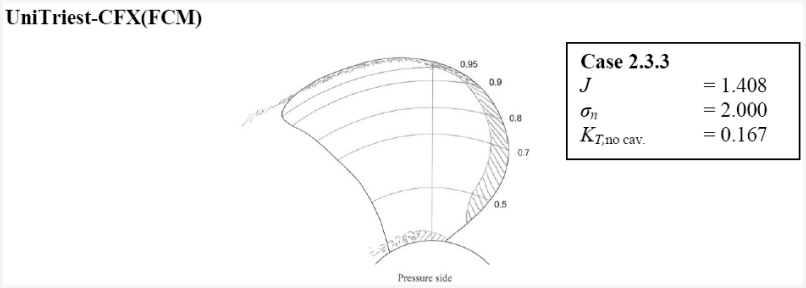

Calculation

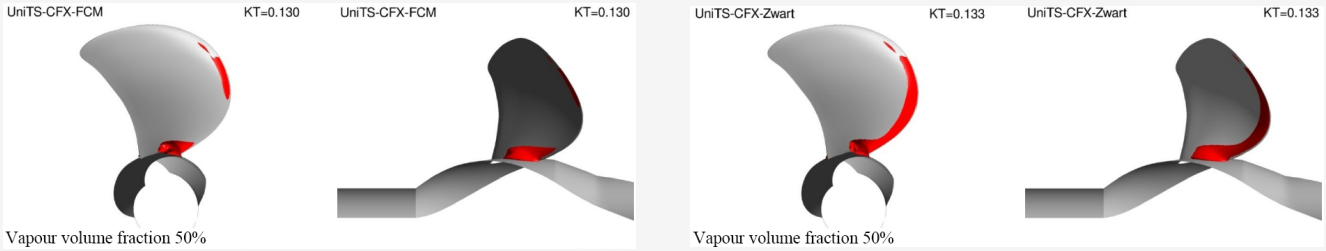

SMP11 - Thrust coefficient

Table 3: Thrust coefficients of cavitating propeller

	case 2.3.1 K_T [-]	case 2.3.2 K_T [-]	case 2.3.3 K_T [-]
Exp. (non-cavitating)	**0.3870**	**0.2450**	**0.1670**
Exp. (cavitating)	**0.3725**	**0.2064**	**0.1362**
Berg-Procal	0.3760		
Cradle-SC/Tetra	0.3750	0.1990	0.1380
CSSRC-Fluent	0.3740	0.1940	0.1320
INSEAN-PFC	0.3570	0.2330	0.1610
SSPA-Fluent	0.3880	0.2050	0.1440
TUHH-FreSCO+	0.3830		0.1440
TUHH-FreSCO+ (small-large coef.)		0.2420 - 0.1370	
UniGenua-Panel	0.3922	0.2369	0.1378
UniGenua-StarCCM	0.3782	0.2035	0.1306
UniTriest-CFX(FCM)	0.3740	0.2030	0.1300
UniTriest-CFX(Kunz)	0.3750	0.2100	0.1330
UniTriest-CFX(Zwart)	0.3730	0.1960	0.1330
VOITH-Comet	0.3852	0.2101	0.1513
VTT-FinFlo	0.3860	0.2020	0.1420

SMP11 - Thrust differences

Table 4: Difference between computed and measured thrust of cavitating propeller

	case 2.3.1 ΔK_T [%]	case 2.3.2 ΔK_T [%]	case 2.3.3 ΔK_T [%]
Berg-Procal	0.94		
Cradle-SC/Tetra	0.67	-3.59	1.32
CSSRC-Fluent	0.40	-6.01	-3.08
INSEAN-PFC	-4.16	12.89	18.21
SSPA-Fluent	4.16	-0.68	5.73
TUHH-FreSCO+	2.82		5.73
TUHH-FreSCO+ (small-large coef.)		17.25 - -33.62	
UniGenua-Panel	5.29	14.78	1.17
UniGenua-StarCCM	1.53	-1.41	-4.11
UniTriest-CFX(FCM)	0.40	-1.65	-4.55
UniTriest-CFX(Kunz)	0.67	1.74	-2.35
UniTriest-CFX(Zwart)	0.13	-5.04	-2.35
VOITH-Comet	3.41	1.79	11.09
VTT-FinFlo	3.62	-2.13	4.26

E779A propeller, non-homogeneous inflow

Experimental setup

E779A, tunnel set-up. Picture taken from [1].

- Operational condition, $J = 0.90$, ($\sigma_n = 4.455$)
  Propeller diameter, $D = 0.227\ m$
  Free-stream inlet velocity, $V = 6.22\ m/s$
  Propeller rotation speed, $n = 30.5\ rps$
  Water density, $\rho_L = 998\ kg/m^3$
  K_T (mean) = 0.175

[1] Salvatore, F, The INSEAN E779A propeller Experimental Dataset.EU-FP6., Project VIRTUE, Deliverable D4.1.3

E779A propeller, non-homogeneous inflow

Numerical setup

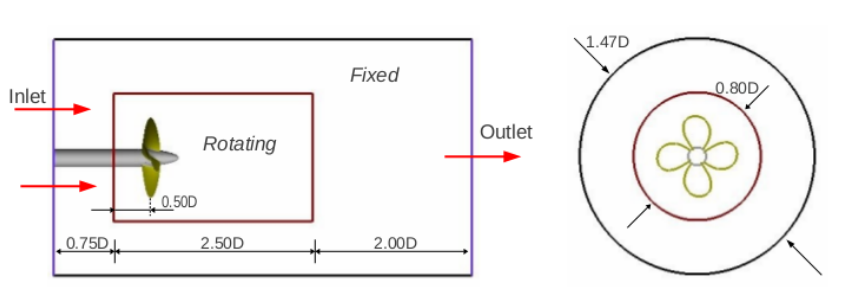

Geometry of the computational domain

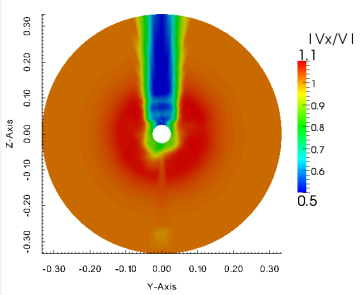

Nominal wake on the Inlet boundary.

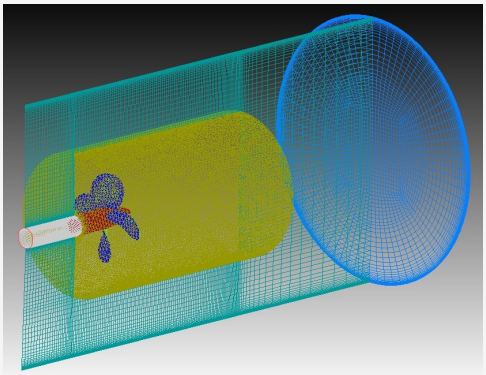

Characteristics of the computational grid

Computational grid		
Rotating		
	number of prisms:	708,000
	number of tetrahedra:	2,012,222
	total number of cells:	2,720,222
Fixed		
	total number of hexahedral cells:	394,839
Total number of cells:		3,115,061

E779A propeller, non-homogeneous inflow

Countours of the axial velocity

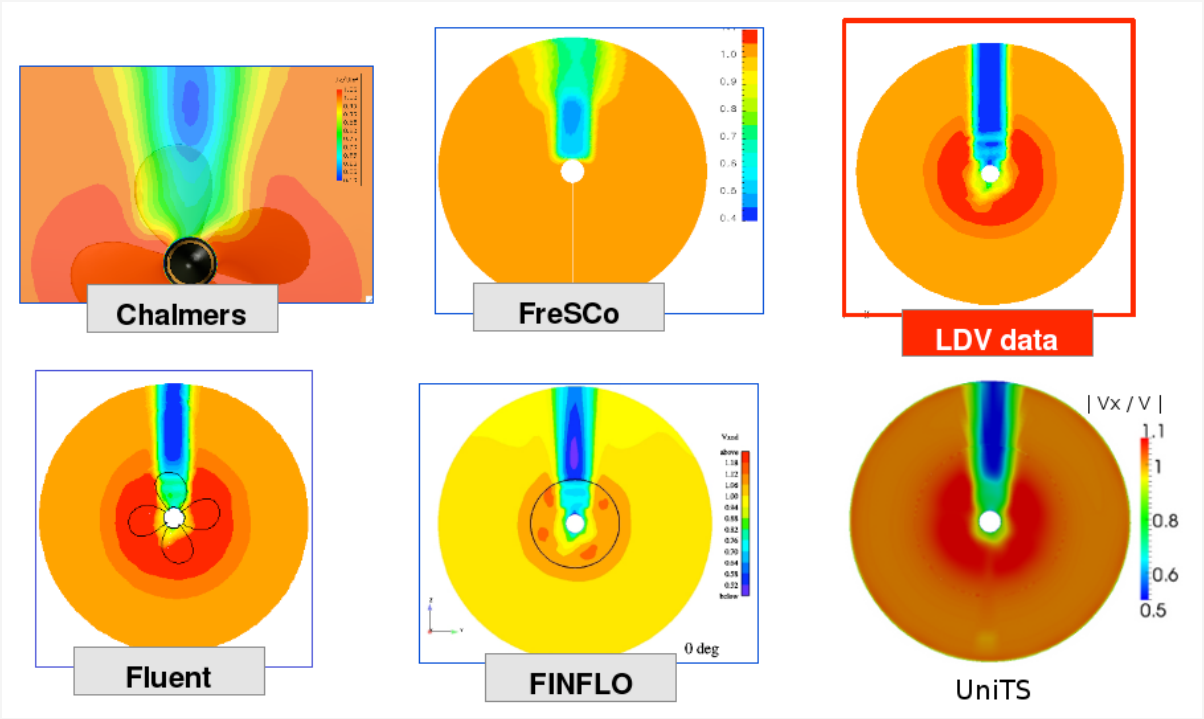

Axial velocity measured/computed in a plane 0.26D upstream of the propeller mid plane. Picture adapted from [2].

International Symposium on Cavitation, smp'09, Trondheim, Norway, pag. 362-371

E779A propeller, non-homogeneous inflow

Contours of Cp=-3.0

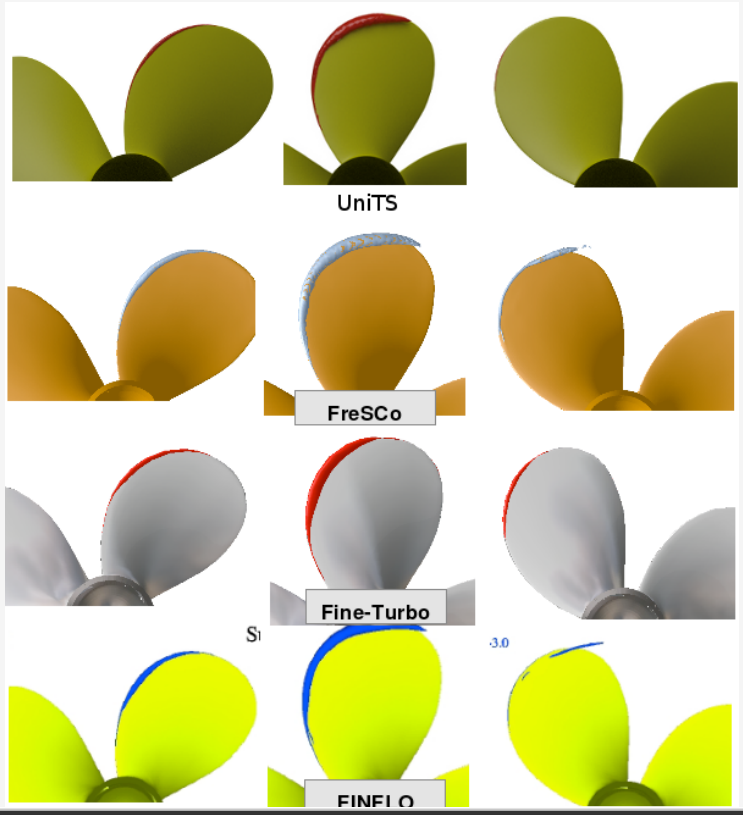

Constant pressure contour for Cp=-3.0 on blade suction side. Picture adapted from [2].

[2] Salvatore, F., and Streckwall, H., and van Terwisga, T., Propeller Cavitation Modelling by CFD-Results from the VIRTUE 2008 Rome workshop, The First

E779A propeller, non-homogeneous inflow

Cavity evolution

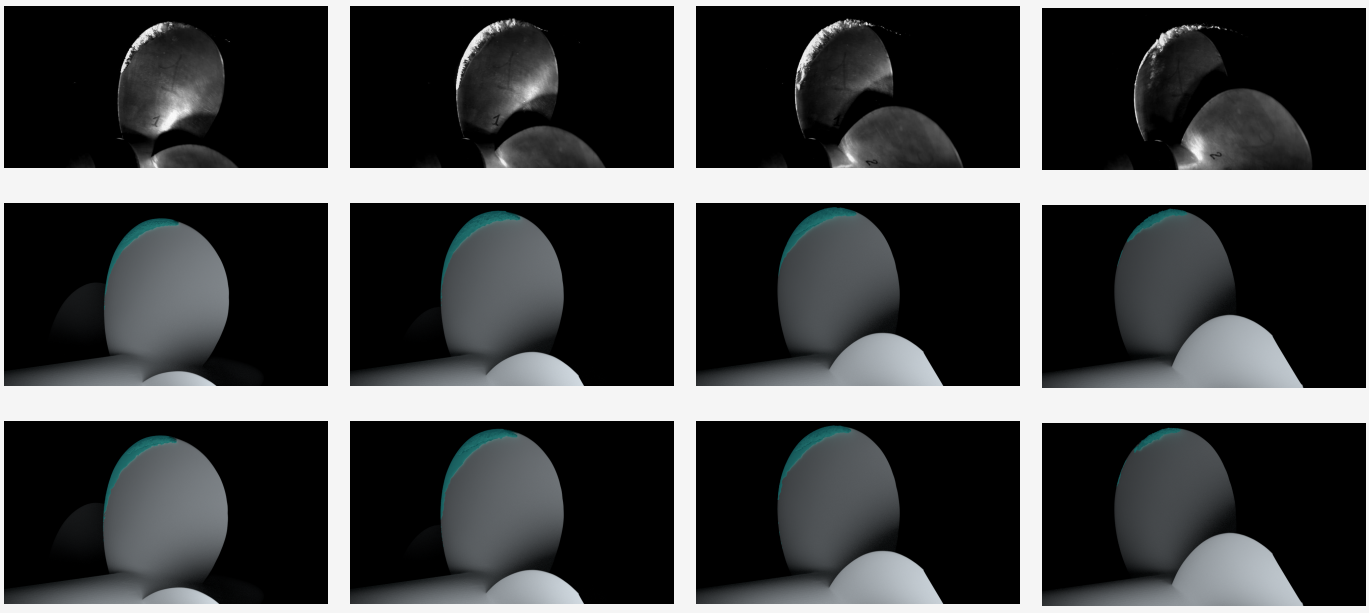

-10° 0° 10° 20°

Cavity evolution with propeller rotation. Experimental data (top). Results obtained with calibrated FCM (middle) and with calibrated Kunz model (bottom).

E779A propeller, non-homogeneous inflow

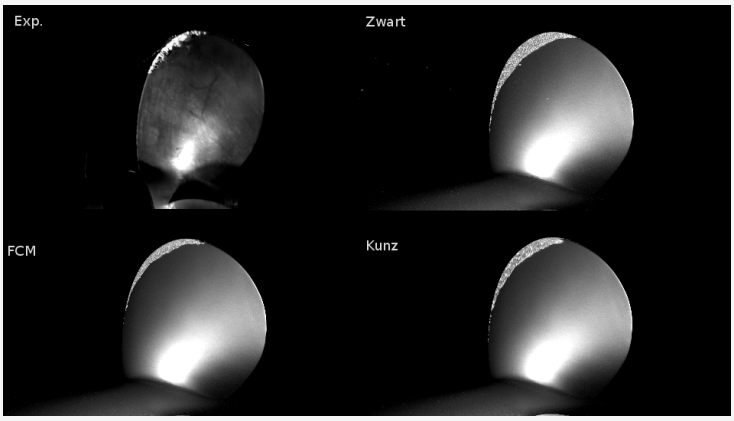

Pelton Turbine - 1

Courtesy of Dr. Dragica Jošt, *Turboinštitut, Ljubljana, SLO*

Experimental model:

Numerical model:

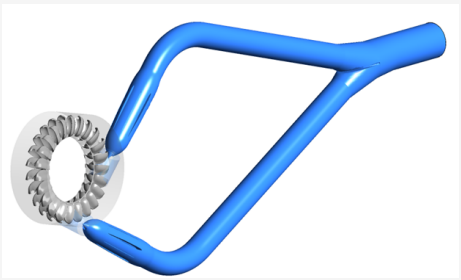

Water jet simulation and related detail:

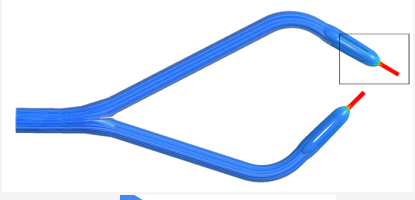

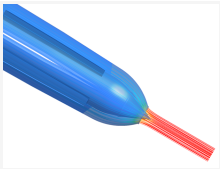

Pelton Turbine - 2

Computational domain and boundary conditions:

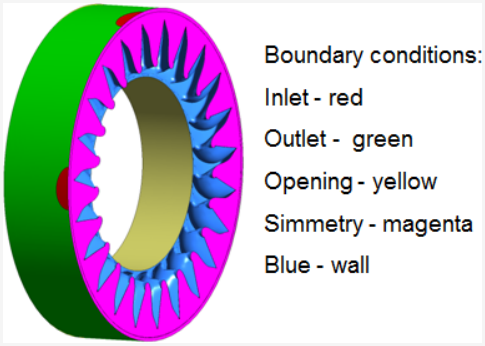

Details of the grid at the entrance and on the surfaces of the buckets:

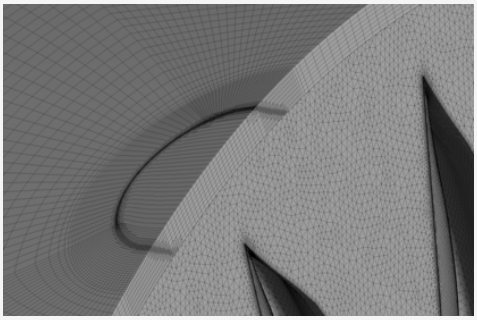

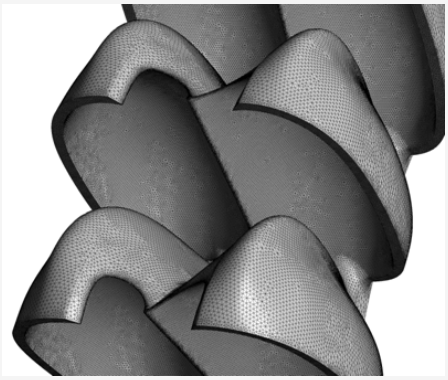

Pelton Turbine - 3

Torque at the shaft during the simulation:

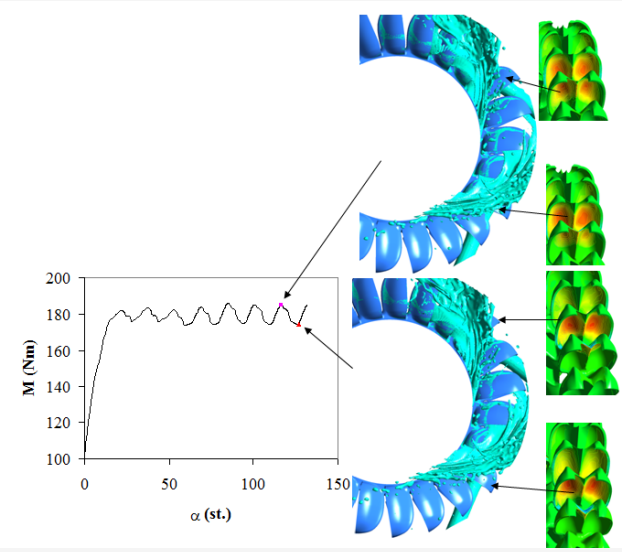

Flow pattern:

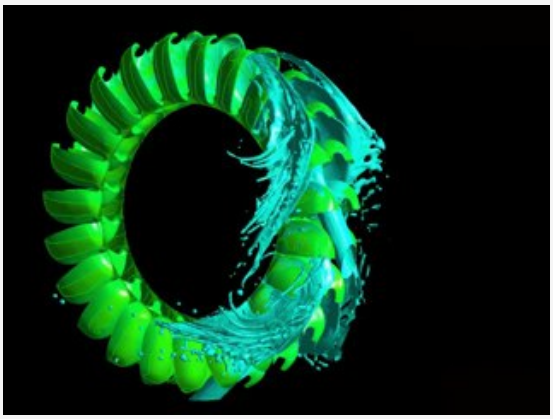

Pelton Turbine - 4

Computed and experimental efficiency:

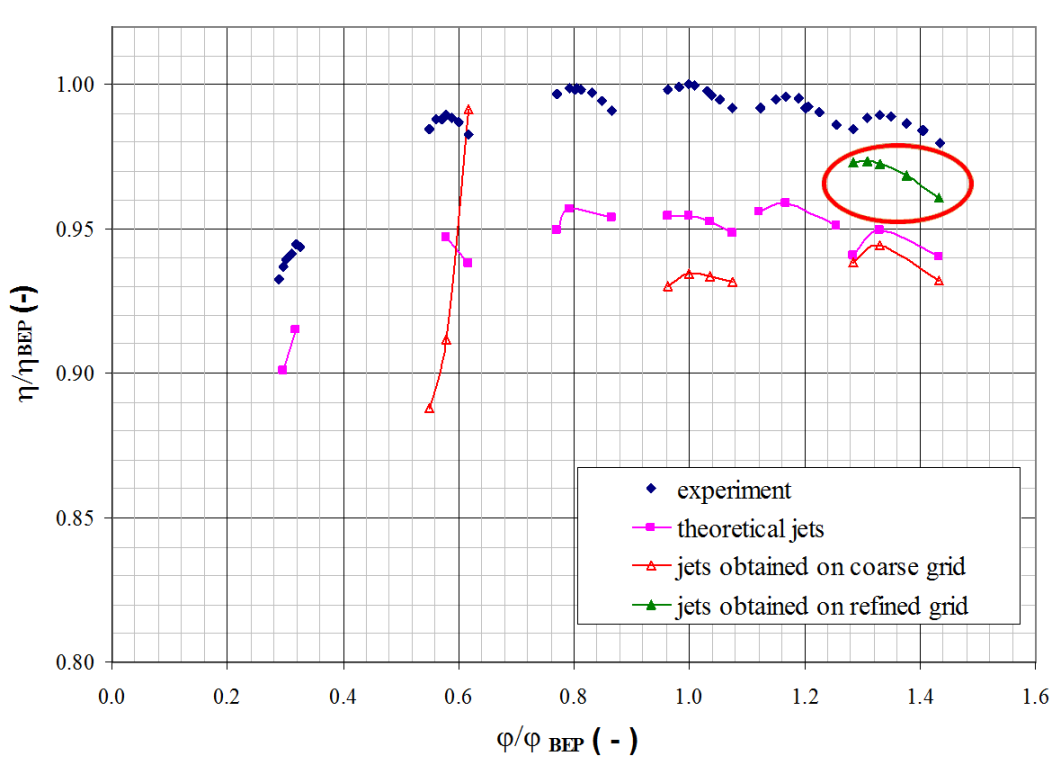

Electromagnetic stirring

Multiphysics Numerical Analysis of Rotary Electromagnetic Stirrers

Definition

Mixing of a liquid metal via rotating electromagnetic fields.

Applications

Casting processes.

Benefits

- promotes heat transfer;
- promotes the growth of equiaxed zones during the solidification process;
- promotes degassing and reduces porosity;
- controls the free surface of the liquid steel in the ingot mold by limiting inclusions.

Improvement of the mechanical properties of steels.

Stirrer

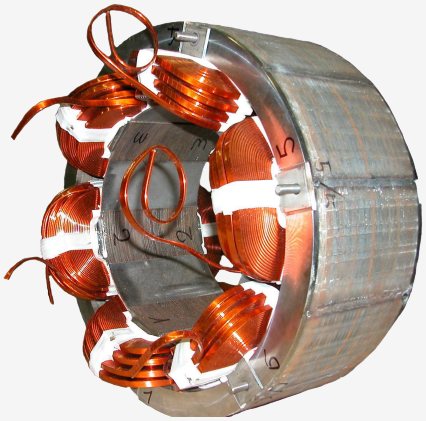

Working principle:

- the rotating field induces currents in the liquid metal;
- the charges, immersed in a magnetic field in relative motion, are subject to the Lorentz force;
- the fluid is set in motion.

Secondary flows - 1

The rotary motion induced by the stirrers in the liquid metal generates important secondary motions.
Let us now consider the two most important cases of stirring:

- Stirring inside a container (aluminium, light alloys);

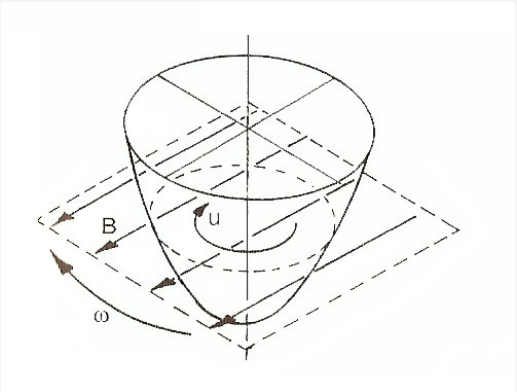

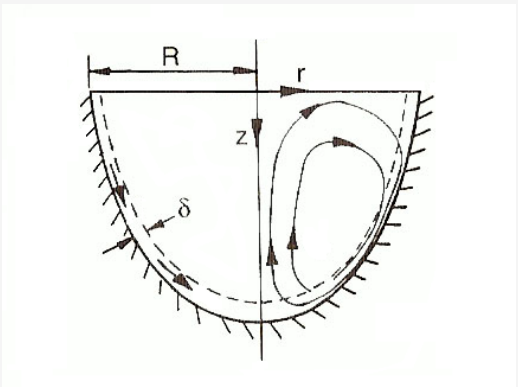

Secondary flows - 2

- Stirring in ingot mould in continuous casting processes.

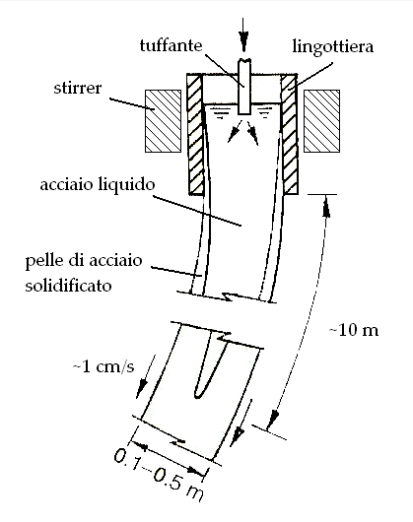

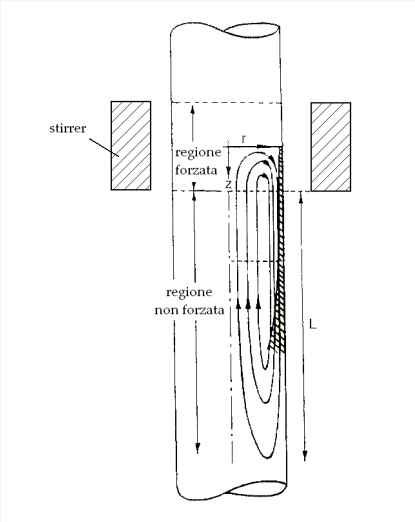

Measurements in the ingot mold are practically impossible: it is necessary to rely on computer simulation tools.

Electromagnetic simulations

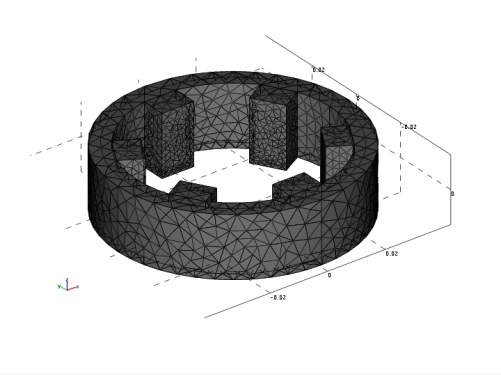

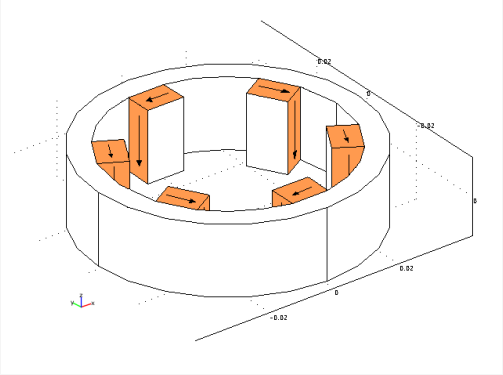

- The stirrer ring and the air are considered as continuous and isotropic bodies;
- The circulation of surface currents is imposed on the faces of the shoes to simulate the windings;
- The magnetic insulator conditions are set on the faces of the *universe*.

$$\left(j\omega\sigma + \omega^2\varepsilon_0\varepsilon_r\right)\mathbf{A} + \nabla \times \left(\mu_0^{-1}\mu_r^{-1}\nabla \times \mathbf{A}\right) = \mathbf{J}^e$$

Magnetic field generated by stirrers

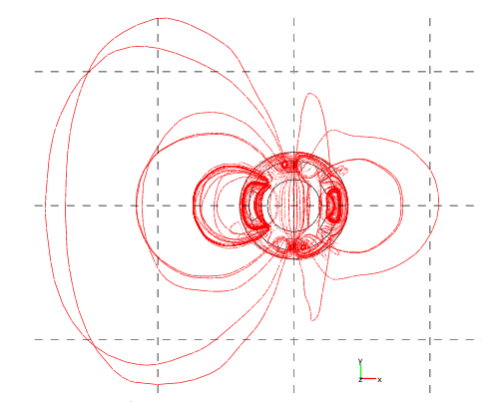

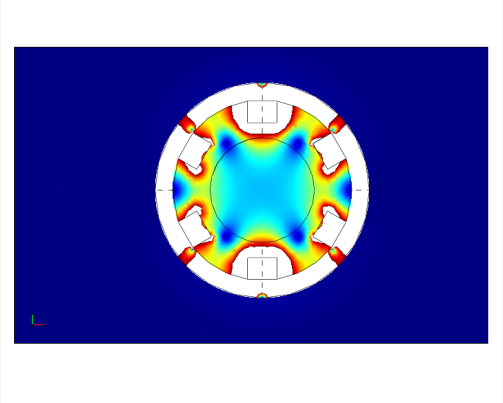

Instantaneous field:

$$B = (real(B_x)^2 + real(B_y)^2 + real(B_z)^2)^{1/2}$$

Time-averaged field:

$$B_{ave} = [0.5 \cdot real(B_x \cdot conj(B_x)) + 0.5 \cdot real(B_y \cdot conj(B_y)) + 0.5 \cdot real(B_z \cdot conj(B_z))]^{1/2}$$

Lorentz forces

Instantaneous value:

$$F_x = real(Ji_y) \cdot real(B_z) - real(Ji_z) \cdot real(By)$$

$$F_y = real(Ji_z) \cdot real(B_x) - real(Ji_x) \cdot real(Bz)$$

$$F_z = real(Ji_x) \cdot real(B_y) - real(Ji_y) \cdot real(Bx)$$

Time-averaged value:

$$F_{x_{ave}} = 0.5 \cdot real(Ji_y \cdot conj(B_z) - Ji_z \cdot conj(B_y))$$

$$F_{y_{ave}} = 0.5 \cdot real(Ji_z \cdot conj(B_x) - Ji_x \cdot conj(B_z))$$

$$F_{z_{ave}} = 0.5 \cdot real(Ji_x \cdot conj(B_y) - Ji_y \cdot conj(B_x))$$

Forces induced in the steel bath

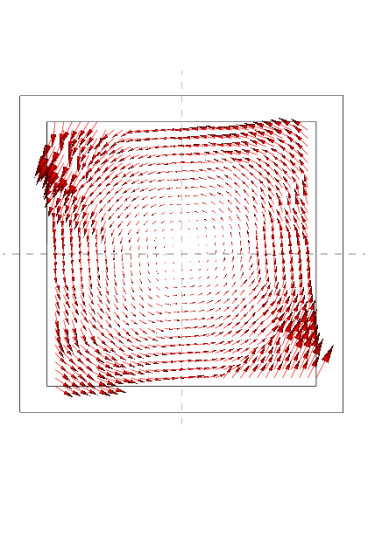

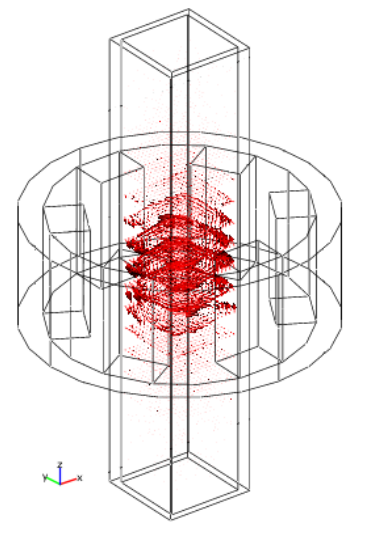

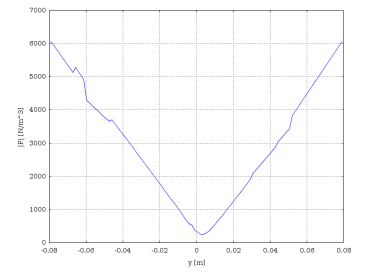

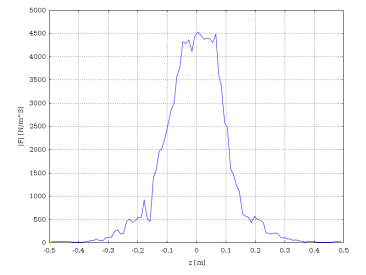

Flow field with the submerged entry nozzle

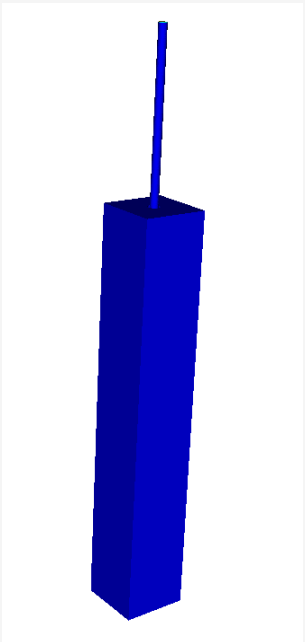

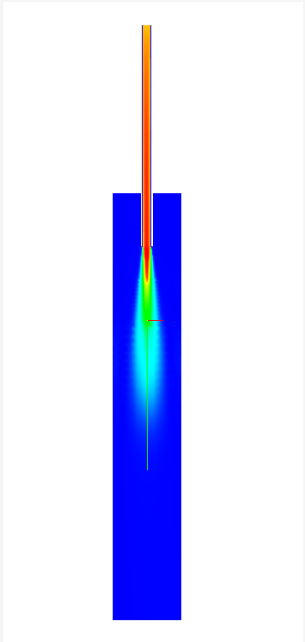

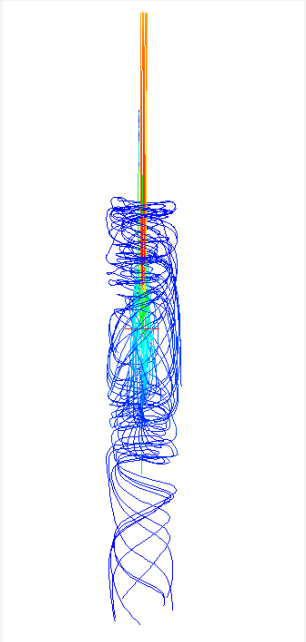

Introduction

Metal Foams

- Porous materials with low densities and tortuous and irregular flow passages
- Pore density 5-100 PPI, porosity 80-97%
- Good candidates for enhancing thermal performances of heat transfer devices

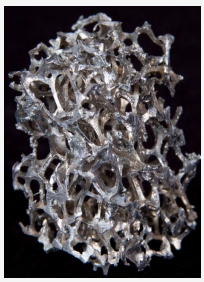

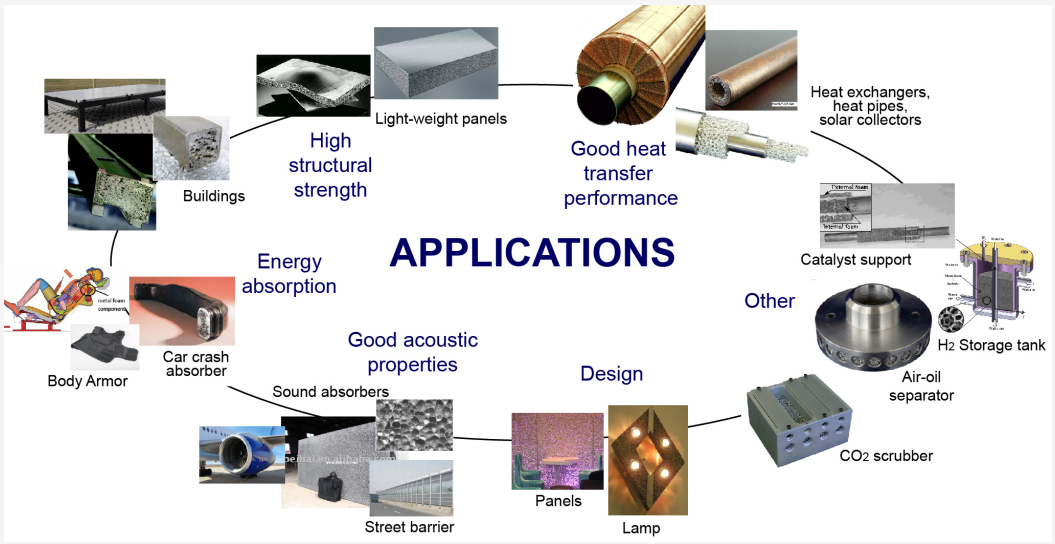

Introduction

Great potential for enhancing thermal performances due to:

- High surface area to volume ratio
- High conductivity of the solid ligaments
- Enhanced flow mixing $\longleftrightarrow$ tortuous and irregular flow passages

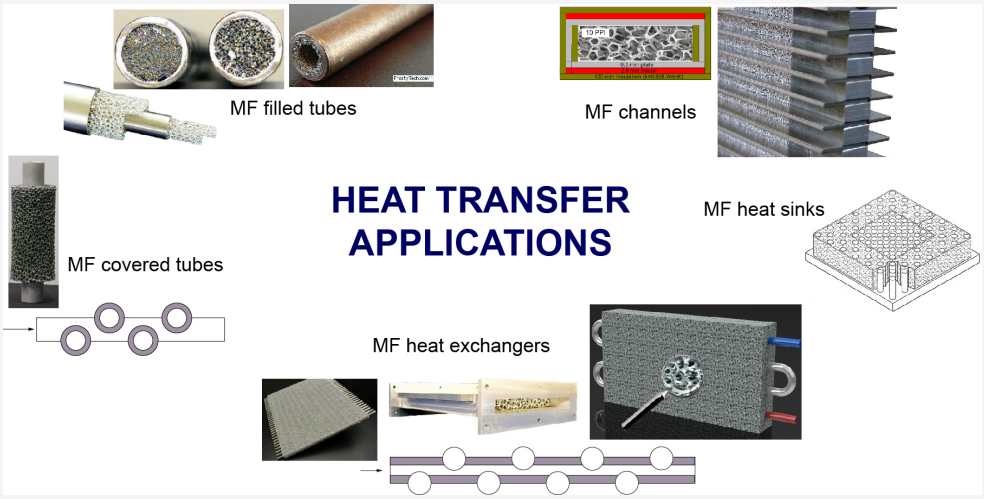

Approaches

For practical applications

It is necessary to characterize and quantify their transport and thermal properties: permeability, K, and effective thermal conductivity, k_{eff}.

- not simple
- information is sometimes scarce

Approaches

- Classical approaches
  - asymptotic solutions
  - empirical correlations
  - unit cell approaches
- CFD simulations
  - simplified models
  - realistic geometries

Many works about porous media, some of which specifically derived for metal foams.

Possible strategies for CFD simulations

- Macroscopic approach
  - Volume Averaging approach
  - the governing equations are volume averaged
  - the porous solid-fluid system is treated as a homogeneous medium
  - the small-scale details are neglected
- Microscopic approach (pore-based approach)
  - Representative Elementary Volume (REV) approach
  - the complex (real or idealized) geometry of the system is considered
  - the small-scale flow details are captured
  - potentially more accurate
  - more costly

REV (Representative Elementary Volume)

- The smallest control volume that gives statistically meaningful local average properties (porosity, permeability, ...)
- When appropriately chosen, addition of extra pores does not change the magnitude of these local properties.

Possible strategies for CFD simulations

Microscopic approach

The microscopic approach is necessary for the quantification of:

- the pressure drop
- the local heat transfer coefficient
- the effective thermal conductivity of the medium

Simplified domains

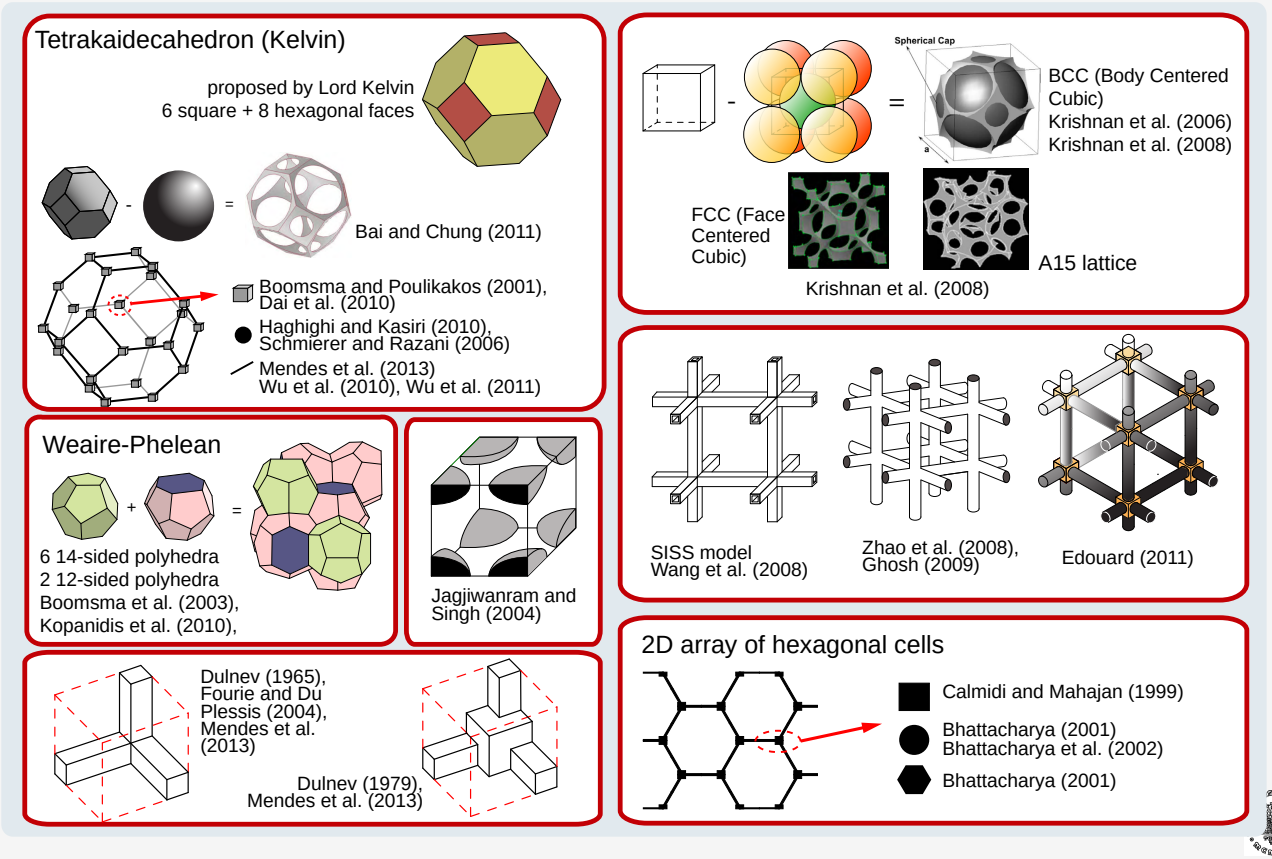

X-ray μ-CT

Non invasive X-ray based method allowing the 3D reconstruction of an opaque sample by illuminating it in different directions.

- An X-ray beam is sent on a sample and the transmitted beam is recorded on a detector
- The sample is made to rotate around its axis
- The total rotational angle depends on both the geometry of the sample and the beam: 180° for nearly parallel beam (e.g., synchrotron) or 360° for cone-beam

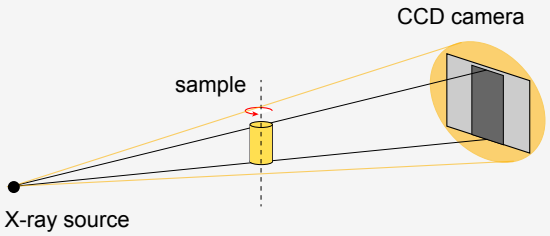

- Several radiographs are recorded at different angles, corresponding to the projection of the linear attenuation coefficient:

$$I = I_0 e^{-\alpha x} \qquad \text{Lambert-Beer Law}$$

I_0: incident intensity radiation intensity
I: emergent (transmitted) radiation intensity
α: linear attenuation coefficient of the material
x: thickness of the medium

- Attenuation depends on both the composition and density of the sample
- The volume can be reconstructed from the set of 2D radiographs with a suitable algorithm

Process

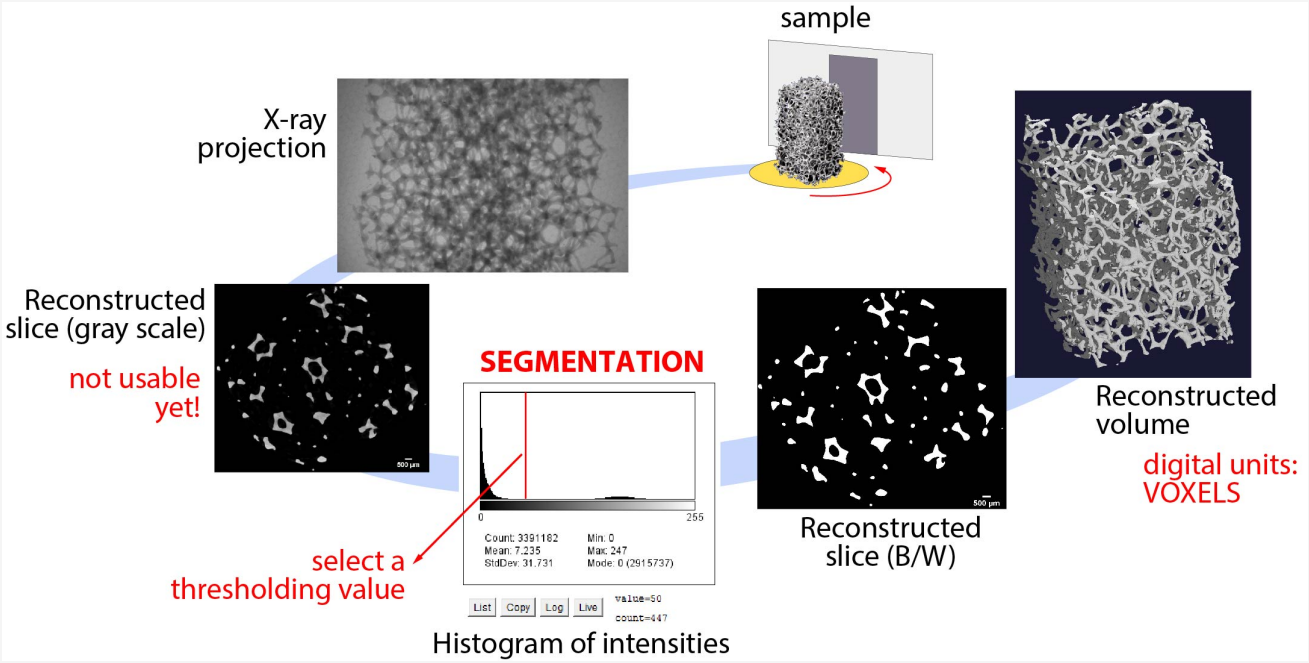

Effect of the threshold value

Threshold = 20 Threshold = 80 Threshold = 140

Synchrotron radiation

> *"Modern laboratory μ-CT setups based on conebeam geometry can produce high-resolution images and due to the small focal spot size of the source they also exhibit phase-contrast effects, but such effects are limited in comparison to synchrotron hard X-ray imaging beamlines."*
>
> Baker et al., Lithos 148 (2012) 262-276.

The use of synchrotron sources can improve significantly the image quality and reduce the scanning time.

- Characteristics:
  - monochromatic beam $\longrightarrow$ no beam hardening effects and high signal-to-noise ratio
  - nearly parallel beam geometry
- Advantages:
  - very high spatial resolutions, even at relatively large sample-to-detector distances
  - more precise definition of the scanned geometry
  - phase-contrast imaging and holotomography can be performed
- However, synchrotron μ-CT is not free of artifacts, e.g., ring artifacts.

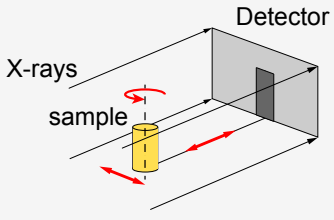

Aluminum foam samples

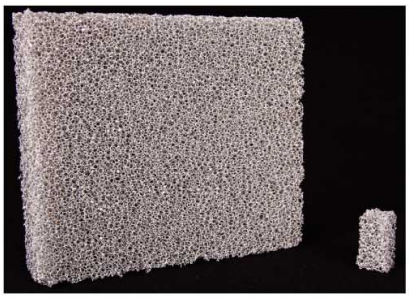

30 PPI

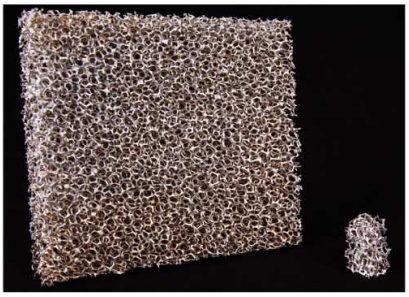

20 PPI

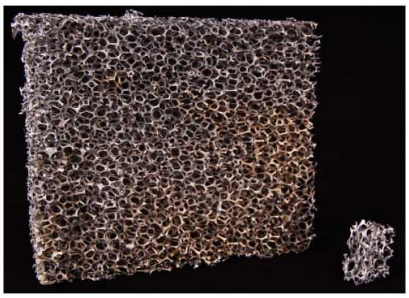

10 PPI

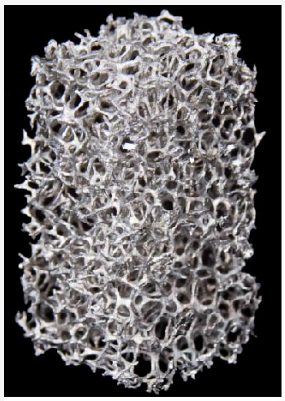

30 PPI

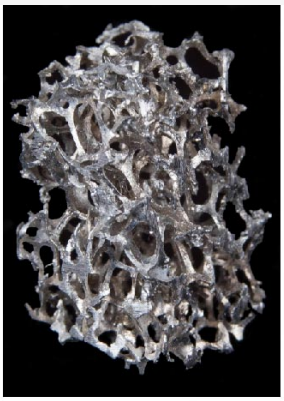

20 PPI

10 PPI

TomoLab Station c/o Elettra Synchrotron Radiation Facility (Trieste)

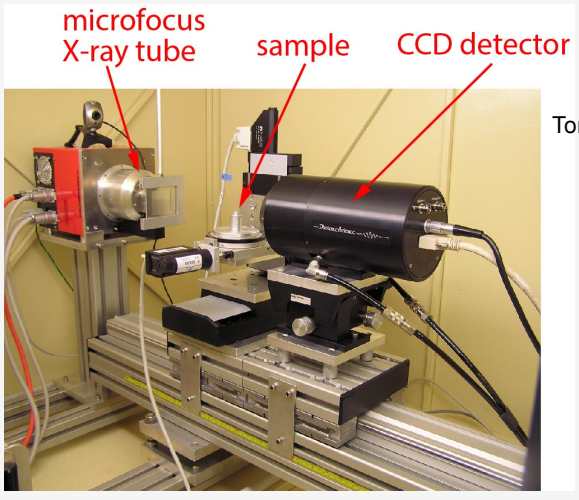

TomoLab Station:

- cone-beam tomographic system
- minimum focal spot size: 5 μm
- energy range 40-130 kV
- maximum current 300 A
- water-cooled 12 bit CCD camera (4008 $\times$ 2672 pixels, effective pixel size 12.5 $\times$ 12.5μm^2)

Experimental conditions:

- voltage: 60 kV, current: 133 μA
- number of recorded projections: 2400 (time: 2h30')
- rotation: 360°
- source-to-sample distance: 80 mm
- source-to-detector distance: 220 mm
- 0.5 mm thick Al filter

Absorption μ-CT at 9.1 μm resolution.

http://www.elettra.trieste.it/lightsources/labs-and-services/tomolab/tomolab.html

Reconstructed volumes

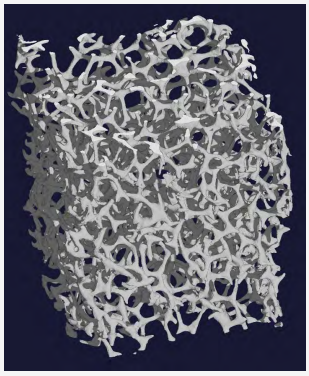
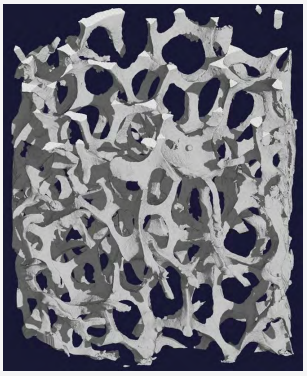
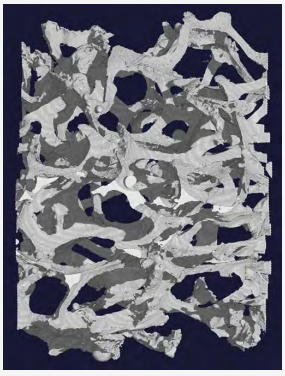

30 PPI | 20 PPI | 10 PPI

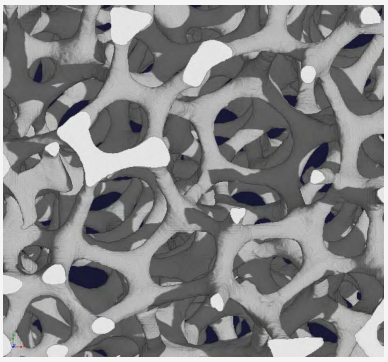
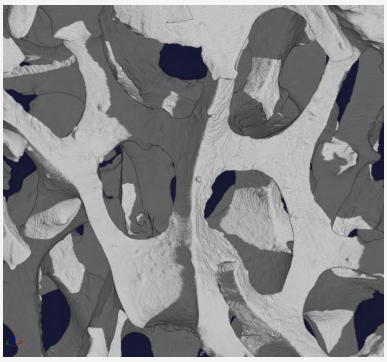
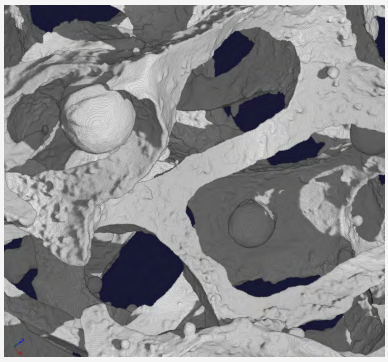

Reconstructed volumes - cont.

The superficial characteristics of the foams vary according to the PPI:

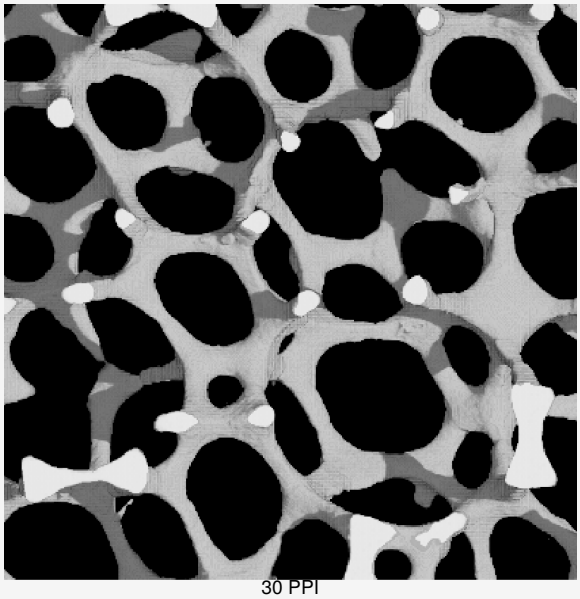
30 PPI

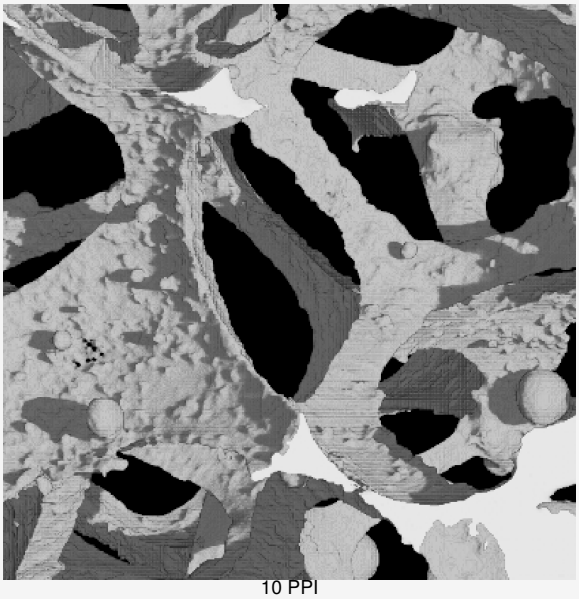
10 PPI

Surface triangulation

- At this point it is necessary to generate a .stl file of the geometry, to be used in the following meshing stage
- VGStudio MAX 2.0 (Volume Graphics)
- In order to generate a usable geometry file, the surface of the mesh must be triangulated

Note

A compromise must be done between:

- accuracy of the triangulation
- size of the exported file

Too heavy files are problematic to handle in the next meshing stage!

↓

This stage introduces an approximation in the process.

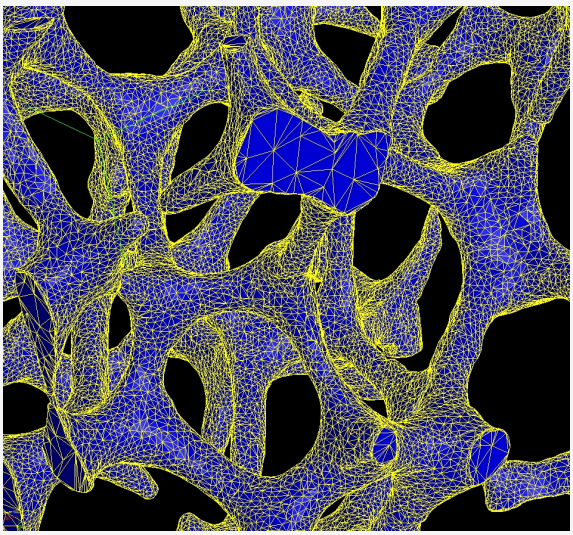

http://www.volumegraphics.com/en/products/vgstudio-max.html

Domains

From each reconstructed volume, a smaller representative cubic volume element was extracted:

- 30 PPI: 548^3 voxels
- 20 PPI: 848^3 voxels
- 10 PPI: 1000^3 voxels

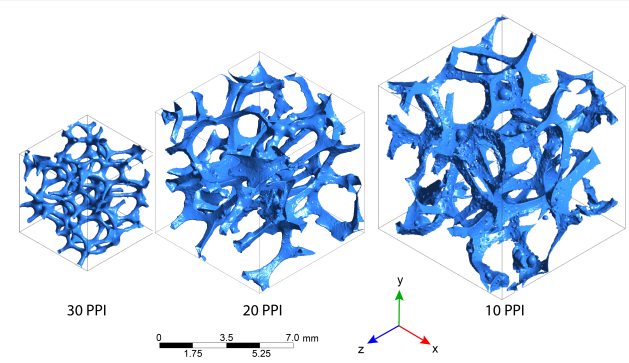

Flow + heat transfer

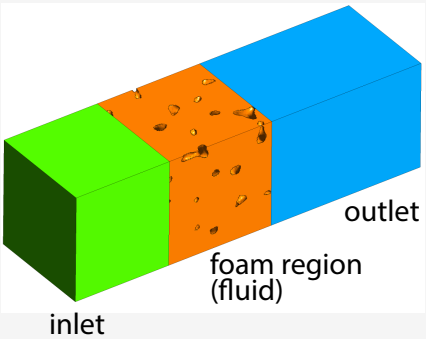

Thermal conductivity

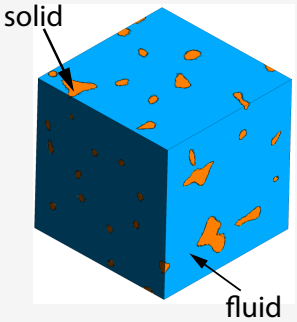

Meshing

- Mesh: geometrically exact, feature-preserving grids
  - central foam region: tetrahedral elements
  - inlet and outlet regions: orthogonal hexahedral mesh
- ANSYS ICEM CFD
- Number of nodes:
  - Flow + Heat transfer (central foam region):
    - 30 PPI: ~1.4×10^6 nodes
    - 20 PPI: ~2.4×10^6 nodes
    - 10 PPI: ~4.1×10^6 nodes
  - Thermal conductivity:
    - 30 PPI: solid ~0.54×10^6, fluid ~0.63×10^6 nodes
    - 20 PPI: solid ~0.83×10^6, fluid ~0.52×10^6 nodes
    - 10 PPI: solid ~1.00×10^6, fluid ~0.65×10^6 nodes

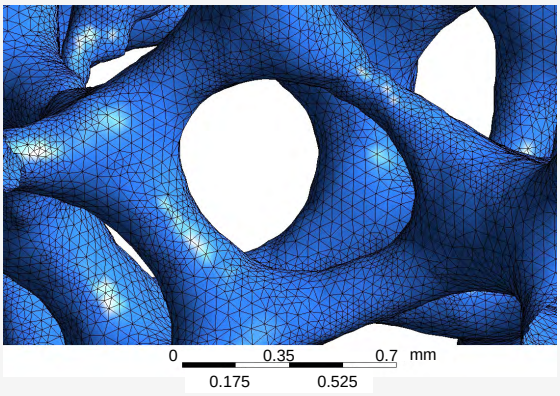

30 PPI

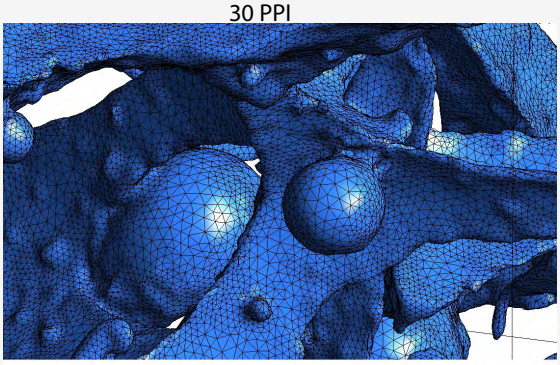

10 PPI

Meshing - cont.

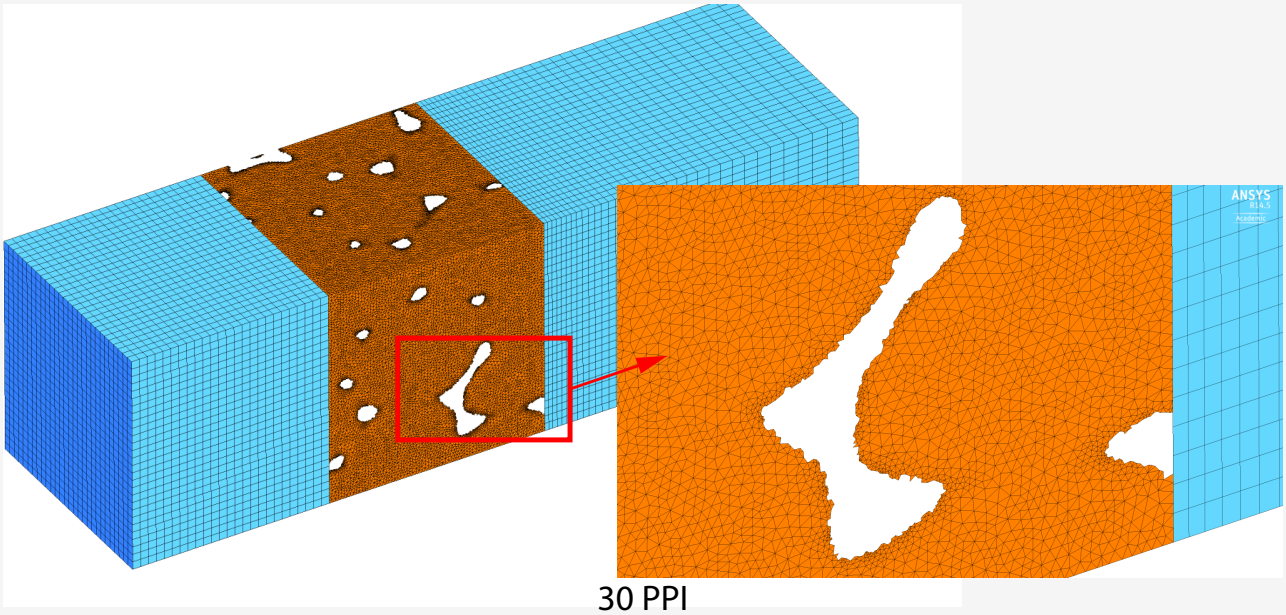

30 PPI

Meshing

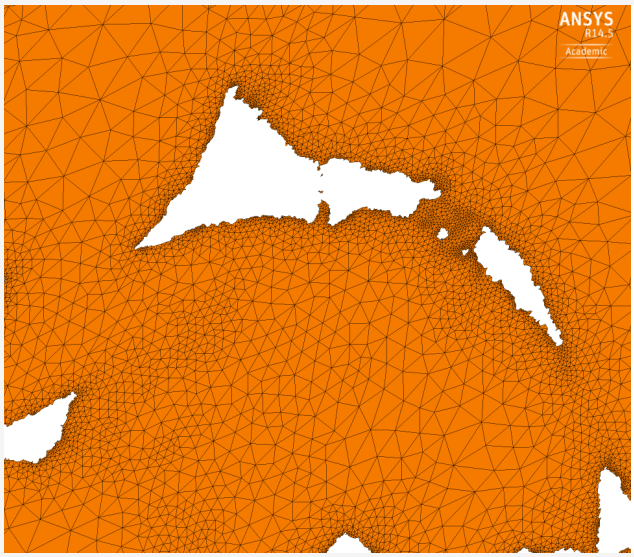

10 PPI

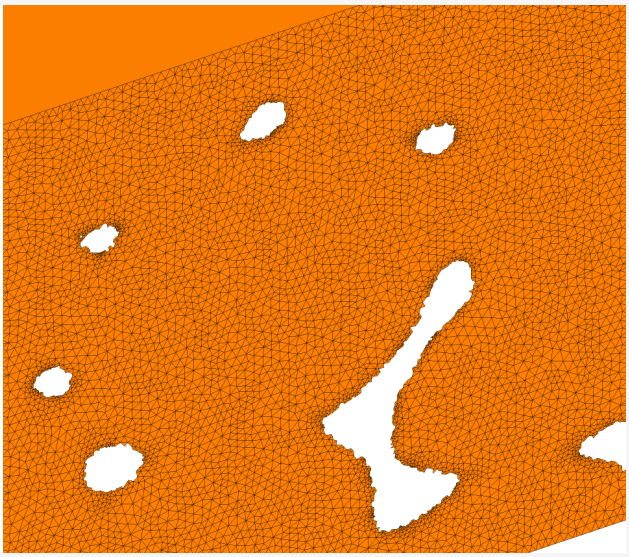

30 PPI

Computational domains

Flow + Heat transfer

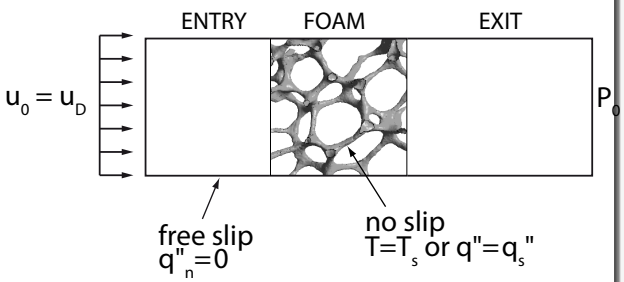

- Air with constant thermophysical properties at 25 °C
- laminar: $Re_p = 1 \div 200$
- steady flow regime
- simulations performed along the three space directions

Thermal conductivity

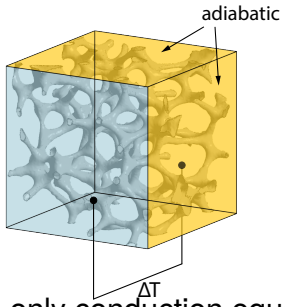

- Solved only conduction equation (no fluid motion), both in the fluid and in the solid, simultaneously
- A fixed (arbitrary) $\Delta T = 10$K set across the domain
- Other faces kept adiabatic
- Both air and water simulated
- k_{eff} estimated along the three space directions

The flow field

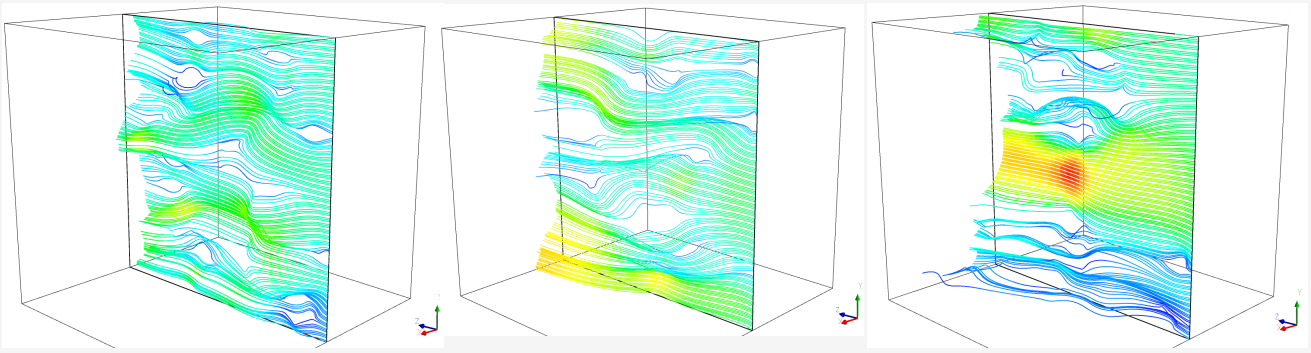

Figure: Flow streamlines at $Re = 10$.

The flow field

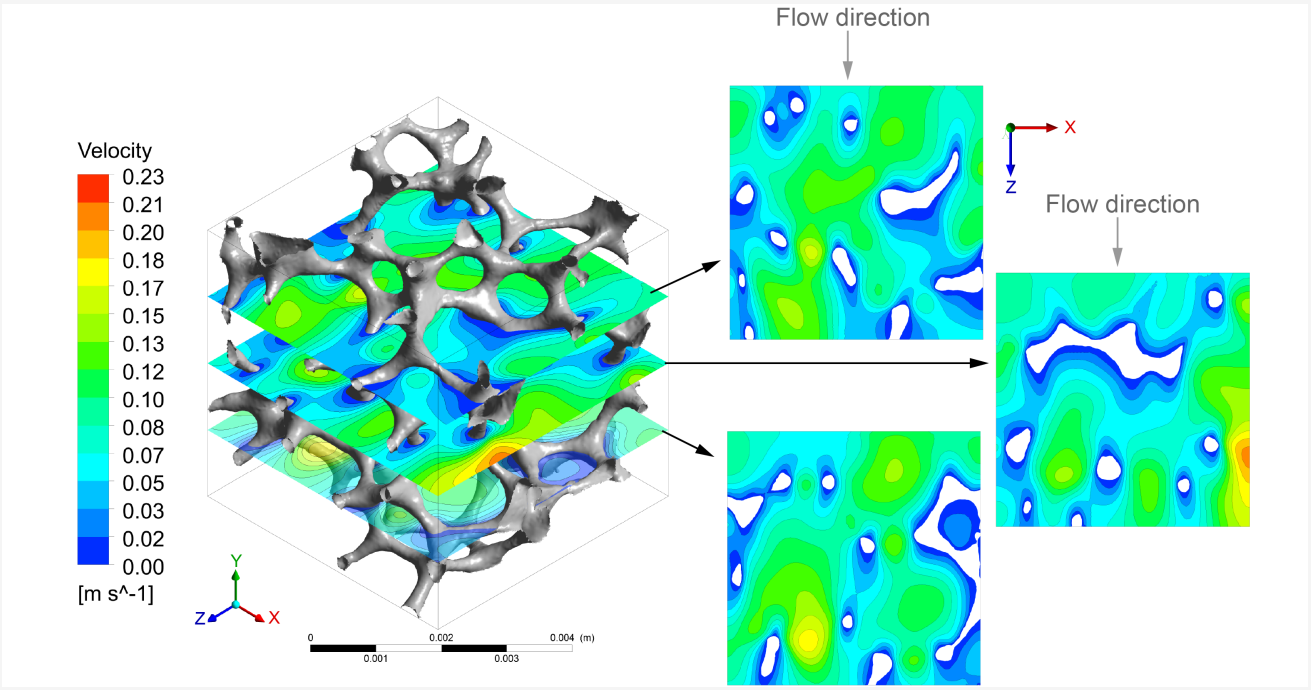

Figure: Visualization of the velocity contours inside the 30 PPI foam at three different sections.

Permeability

$$\frac{\nabla P \cdot d_p^2}{\mu \cdot u_D} = -\frac{d_p^2}{K} - C d_p Re$$

	30 PPI $\varepsilon = 0.929$		20 PPI $\varepsilon = 0.935$		10 PPI $\varepsilon = 0.944$	
	K$\times 10^7$	C	K$\times 10^7$	C	K$\times 10^7$	C
x	0.872	389.0	2.694	240.3	2.906	218.6
y	0.859	392.9	2.342	250.3	3.058	255.2
z	0.858	370.6	2.306	257.6	3.234	187.9
Av.	0.863	384.2	2.477	249.4	3.066	220.6

Table: Values of permeability K [m^2] and of the Dupuit-Forchheimer coefficient C [m^{-1}], for the three foam samples. $Av.$ refers to the value averaged along the three directions. ε is the porosity of the foam.

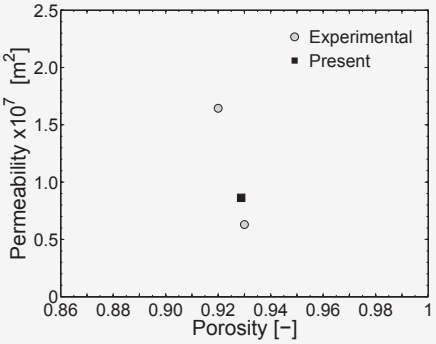

30 PPI

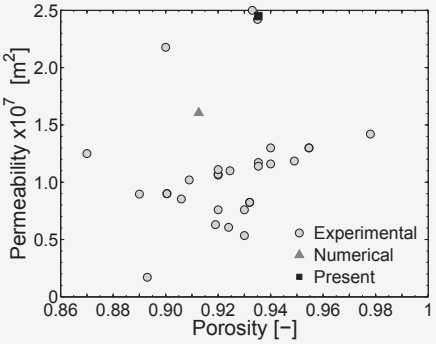

20 PPI

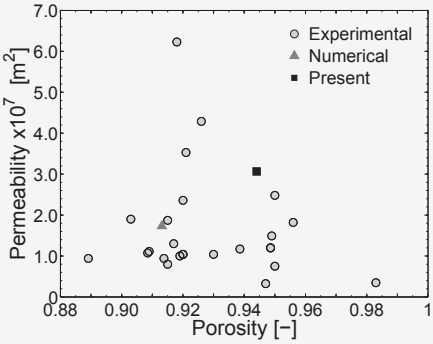

10 PPI

Effective thermal conductivity

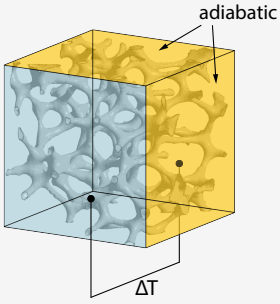

- Solved only conduction equation (no fluid motion), both in the fluid and in the solid, simultaneously
- A fixed (arbitrary) $\Delta T = 10$K set across the domain
- Other faces kept adiabatic
- Both air and water simulated
- k_{eff} estimated along the three space directions

$$k_{\text{eff}} = \frac{-\int \mathbf{J} \cdot d\mathbf{A}}{\frac{\partial T}{\partial x_i} A} = \frac{-\left(\int_s \mathbf{J} \cdot d\mathbf{A}_s + \int_s \mathbf{J} \cdot d\mathbf{A}_f\right)}{\frac{\partial T}{\partial x_i}(A_s + A_f)}$$

J: heat flux
$d\mathbf{A}$: outward pointing area vector
s: refers to the solid
f: refers to the fluid

Results

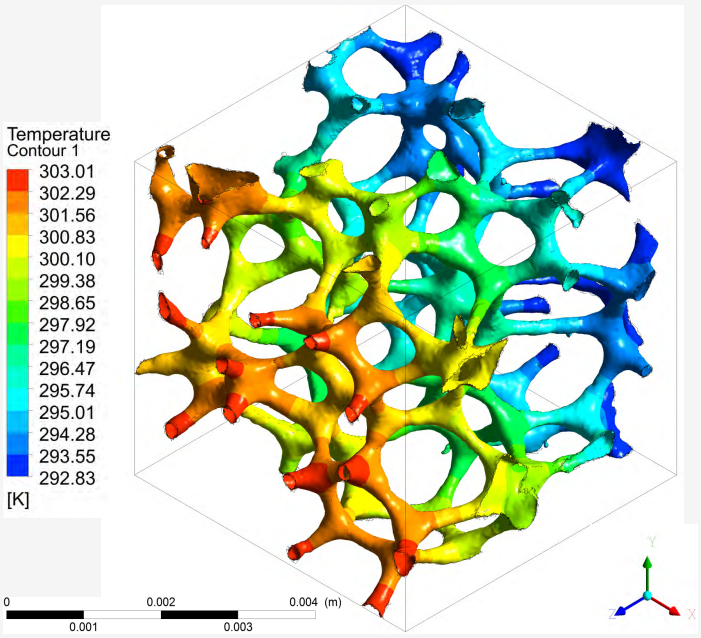

Figure: 30 PPI, temperature gradient applied along the z direction.

Results

PPI	Porosity	air	water
10	0.944	3.49	4.13
20	0.927	4.57	5.27
30	0.929	5.31	5.99

- k_{eff} with water is slightly larger than that with air
- the thermal conductivity of the fluid influences, but not in a significant way, k_{eff}

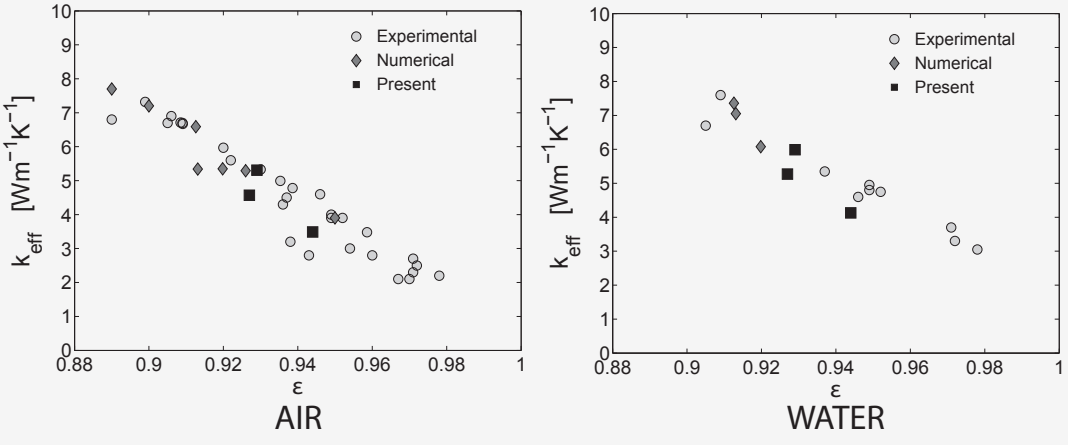

Example of application

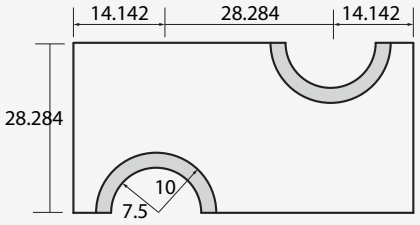

Porosity	ε	0.929
Permeability	K	8.631×10^{-6} m^2
Form drag coefficient	C	384.2×10^{3} m^{-1}
Effective thermal conductivity	k_{eff}	W/(m K)

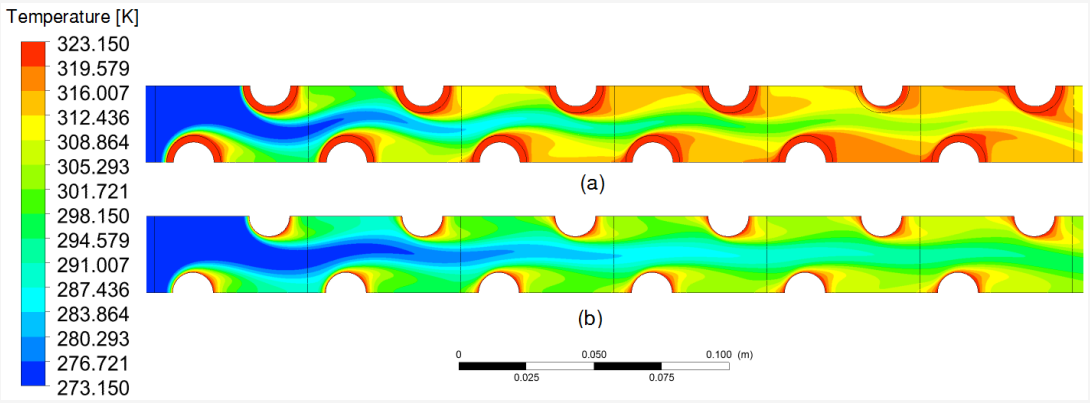

COATED

$\Delta T = 37.5$ K

+ 41%

NOT COATED

$\Delta T = 26.6$ K

Example of application

The heat transfer enhancement is gained at the expense of a triple pressure loss

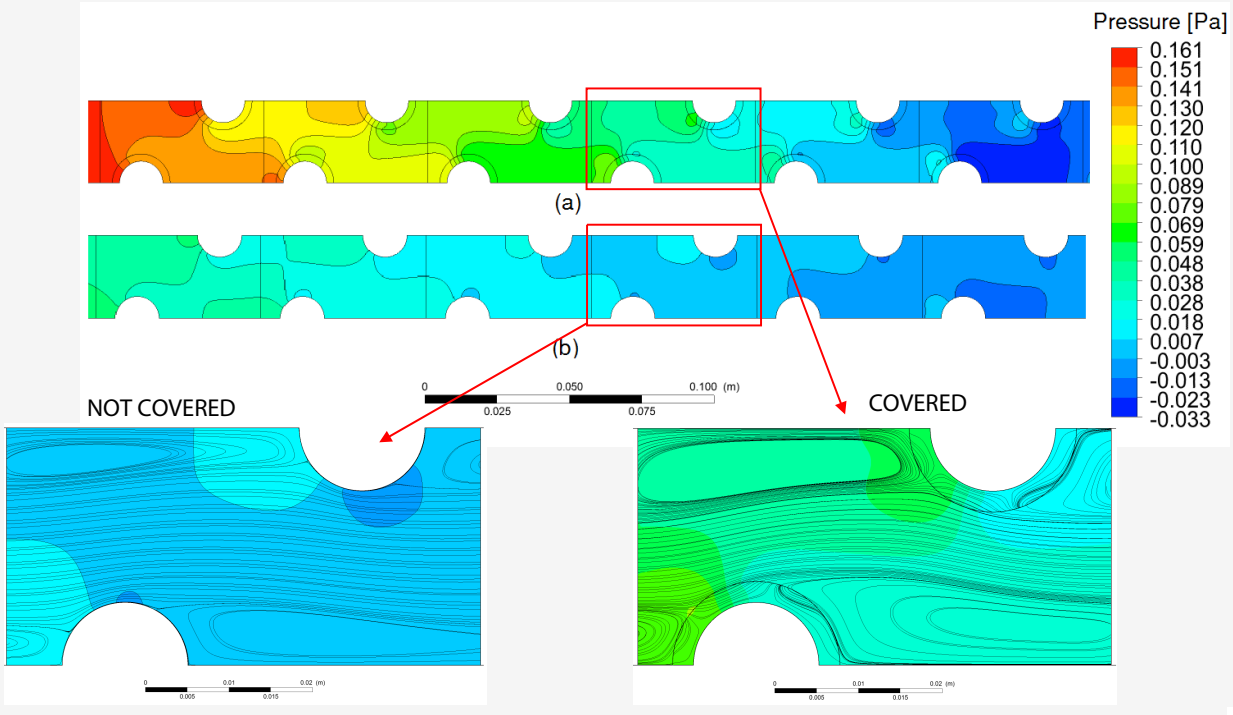

Fires and smoke

By courtesy M. Manzan

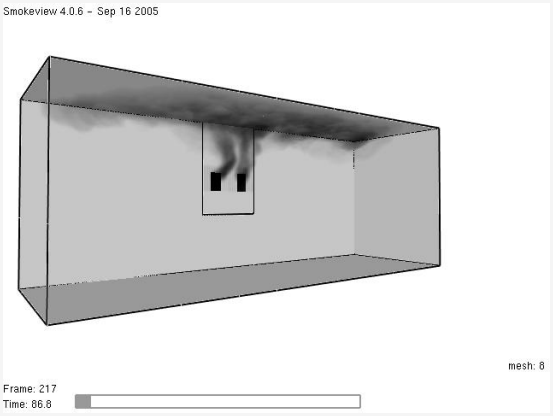

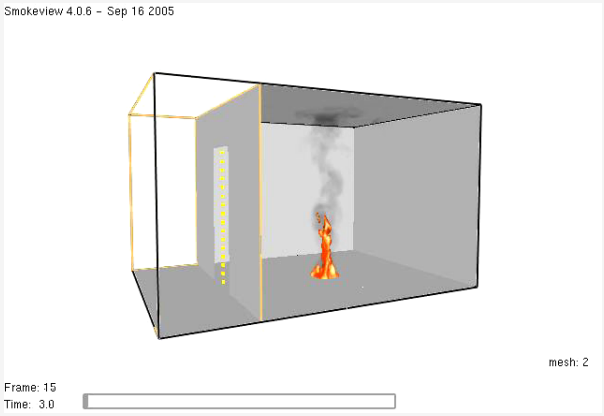

CFD in Cardiovascular Medicine

Review

OPEN ACCESS

Computational fluid dynamics modelling in cardiovascular medicine

Paul D Morris,[1,2,3] Andrew Narracott,[1,2] Hendrik von Tengg-Kobligk,[4] Daniel Alejandro Silva Soto,[1,2] Sarah Hsiao,[1] Angela Lungu,[1,2] Paul Evans,[1,2] Neil W Bressloff,[5] Patricia V Lawford,[1,2] D Rodney Hose,[1,2] Julian P Gunn[1,2,3]

▸ Additional material is published online. To view please visit the journal (http://dx.doi.org/10.1136/heartjnl-2015-308044)

[1]Department of Cardiovascular Science, University of Sheffield, Sheffield, UK
[2]Insigneo Institute for In Silico Medicine, Sheffield, UK
[3]Department of Cardiology, Sheffield Teaching Hospitals NHS Trust, Sheffield, UK
[4]University Institute for Diagnostic, Interventional and Pediatric Radiology, University Hospital of Bern, Inselspital, Bern, Switzerland
[5]Faculty of Engineering & the Environment, University of Southampton, Southampton, UK

Correspondence to
Dr Paul D Morris, Medical Physics Group, Department of Cardiovascular Science, University of Sheffield, The Medical School, Beech Hill Road, Sheffield S102RX, UK; paulmorris@doctors.org.uk

Received 23 April 2015
Revised 20 September 2015
Accepted 21 September 2015
Published Online First
28 October 2015

ABSTRACT
This paper reviews the methods, benefits and challenges associated with the adoption and translation of computational fluid dynamics (CFD) modelling within cardiovascular medicine. CFD, a specialist area of mathematics and a branch of fluid mechanics, is used routinely in a diverse range of safety-critical engineering systems, which increasingly is being applied to the cardiovascular system. By facilitating rapid, economical, low-risk prototyping, CFD modelling has already revolutionised research and development of devices such as stents, valve prostheses, and ventricular assist devices. Combined with cardiovascular imaging, CFD simulation enables detailed characterisation of complex physiological pressure and flow fields and the computation of metrics which cannot be directly measured, for example, wall shear stress. CFD models are now being translated into clinical tools for physicians to use across the spectrum of coronary, valvular, congenital, myocardial and peripheral vascular diseases. CFD modelling is apposite for minimally-invasive patient assessment. Patient-specific (incorporating data unique to the individual) and multi-scale (combining models of different length- and time-scales) modelling enables individualised risk prediction and virtual treatment planning. This represents a significant departure from traditional dependence upon registry-based, population-averaged data. Model integration is progressively moving towards 'digital patient' or 'virtual physiological human' representations. When combined with population-scale numerical models, these models have the potential to reduce the cost, time and risk associated with clinical trials. The adoption of CFD modelling signals a new era in cardiovascular medicine. While potentially highly beneficial, a number of academic and commercial groups are addressing the associated methodological, regulatory, education- and service-related challenges.

Open Access
Scan to access more free content

CrossMark

To cite: Morris PD, Narracott A, von Tengg-Kobligk H, *et al*. *Heart* 2016;**102**:18–28.

INTRODUCTION
Computational fluid dynamics (CFD) is a well-established tool used in engineering, in many areas of which it has become the primary method for design and analysis. Bioengineers have adopted CFD to study complex physiological flows and have demonstrated their potential.[1] There is increasing interest in applying these methods in cardiovascular medicine.[2 3] CFD-based techniques are being used to build complex computer representations (in silico models) of the cardiovascular system in health and disease. CFD modelling is a new field within cardiovascular medicine, enhancing diagnostic assessment, device design and clinical trials. It can predict physiological responses to intervention and compute previously unmeasurable haemodynamic parameters.[4] As CFD modelling continues to translate into clinical tools, it is important that clinicians understand the principles, benefits and limitations of these techniques. This article explores these topics using state-of-the-art examples in key clinical areas, highlighting applications likely to impact clinical practice within the next 5 years (table 1).

WHAT IS CFD?
CFD is a specialist area of mathematics and a branch of fluid mechanics. It is used in the design of many safety-critical systems, including aircraft and vehicles, by solving differential equations to simulate fluid flow. A glossary of uesful terms is provided in table 2.

For incompressible flows, almost all CFD analyses solve the Navier-Stokes and continuity equations which govern fluid motion. These equations are non-linear, partial differential equations based upon the principle of conservation of mass and momentum. Simplification of these equations yields familiar formulae (eg, those of Bernoulli and Poiseuille); but for complex geometries analytical solutions are not possible, so specialised software applications (CFD solvers) calculate approximate numerical solutions. Non-linearity, due to convective fluid acceleration, makes this challenging, especially in three dimensional (3D) models; so CFD analyses require significant computational power and time.

CFD MODEL COMPLEXITY
The applications reviewed in this paper focus on 3D CFD analyses of local regions of the vasculature because this is where promising applications are beginning to translate and impact upon clinical medicine. There is a long history of simplification of the governing equations to lower spatial dimensions. Table 3 summarises the relationship between these approaches and provides clinical examples of their use.

2D analyses typically assume symmetry of the solution about the central axis, 1D models capture variation of the solution along the axial direction only, and 0D representations lump the behaviour of vascular regions into a model with no spatial dimensions, hence the term 'lumped-parameter models'. Due to the breadth of the literature covering application of these techniques to cardiovascular haemodynamics, the interested reader is referred to recent reviews of the state-of-the-art.[4 5 46]

CFD in Cardiovascular Medicine - cont.

Table 1 Summary of CFD modelling applications in cardiovascular medicine

Area	Clinical applications	Data and evidence	Potential clinical impact	Limitations and challenges	References
Coronary artery disease and physiology	Models based upon coronary angiography (CT /invasive) to compute physiological coronary lesion significance less invasively	Multiple trials demonstrating broadly good agreement between standard and CFD-derived FFR (vFFR). Lesion significance established in ~80–90%	Widened access to the benefits of physiological lesion assessment; vFFR lacks the practical limitations that restrict use of the invasive technique. Virtual stenting enables planning and selection of optimal treatment strategy	Accurate vessel reconstruction and patient-specific tuning of the model boundary conditions (especially those of myocardial resistance)	5 6 7 8
Valve prostheses	Evaluation and optimisation of prosthetic valve design from a haemodynamic perspective	Included in the design dossier given to RA for approval before use in humans. Third party, comparative studies are in engineering literature	CFD modelling enables the best design, yielding the optimal haemodynamics and lowest achievable risk of design-related thrombosis and thromboembolism	Dependence upon validity of models to interpret fluid stresses in terms of thrombogenic/haemolytic potential. Primarily relates to mechanical valves. Tissue valve leaflets remain challenging to model	9 10 11
Native valve haemodynamics in health and disease	Non-invasive computation and quantification of trans-valvular pressure drop and regurgitant fraction from CT imaging	Accurate 3D simulations in patient-specific models with valves in open and closed states to predict transvalvular dynamics in diseased states	Improved objective assessment and surveillance of valve disease from non-invasive imaging data	Requires high quality 3D images of valve orifice—not routinely generated. Balancing the requirement for complex dynamic simulation (FSI) vs simpler models (valve open/closed)	12 13
Aortic aneurysm	Provides quantitative haemodynamic data for non-invasive imaging to emphasise the significance of findings. Virtual therapy simulation/predictions	No published outcome trials, only single centre experiences and small cohorts using different boundary condition and computational methods	To better predict aneurysm progression and risk of rupture. Prediction of putative therapeutic effects. Individualised care and reduction in costs for unnecessary follow-up imaging and visits	Impact of low image contrast structures of aortic aneurysm (eg, wall, thrombus) as well as wall motion needs to be further assessed. CFD alone is probably limited and needs to be complemented by, for example, FSI	3 14 15 16
Aortic dissection	Pathophysiological conditions in true and false lumen computed from non-invasive boundary conditions (CT and MRI +PC). Effects of virtual therapy.	No published outcome trials, only single centre experiences and small cohorts using different boundary conditions and computational methods	Computed pressure and flow conditions used to guide (semi-) invasive therapeutic procedure decisions. Physiological effects of therapies can be simulated and better predicted	Significant early and late re-modelling of the dissected wall. Entry, re-entry and communication channels create a complex computational scenario. CFD alone might be limited. A potential role for FSI	17 18 19
Stent design	Prediction of WSS and related metrics that influence endothelial function and NH due to stent-induced haemodynamic disturbance	Turbulent or disturbed laminar flow reduces WSS stimulating adverse vessel remodelling. NH preferentially accumulates in these regions	Not possible to measure arterial WSS in vivo, especially in the vicinity of stent struts post-PCI. Modelling provides detailed analysis of flow, and the influence of stent design through patient-specific reconstructions, enabling the optimal stent design to be achieved	High resolution imaging, vessel reconstruction and boundary conditions are challenging. CFD simulations demand fine computational meshes and time-resolved pulsatility. Run-times are long, even with high performance computing	20 21 22 23 24 25 26 27
Cerebral aneurysm	Prediction of intra-aneurysmal flow, stasis, jet impingement and WSS from MRI and CT cerebral angiography data	Published data on association between WSS, aneurysm initiation, growth, and potentially rupture	Detailed, individualised haemodynamic analysis with potential for risk prediction. Impact of putative treatments on local haemodynamics evaluated in silico	Difficulty interpreting complex and detailed WSS results. Understanding how results translate to rupture risk. Validation of rupture predictions—a rare event	4 28 29
Pulmonary hypertension (PH)	Greater insights into complex PH physiology. Increasing interest in non-invasive diagnosis and monitoring of response to treatment	Models based on MR flows demonstrated to differentiate between healthy volunteers and to stratify PH subcategories	Imaging-based modelling of pulmonary haemodynamics can reduce the requirement for right heart catheterisation. Models show association between reduced WSS and invasive PH metrics. PH subtype characteristics simulated to understand the structural changes contributing to increased PAP	Spatial resolution of imaging and segmentation protocols. The use of a pressure surrogate measure. The presence of many outlets requiring many measurements to tune the outflow boundary conditions	30 31 32 33
Arterial wall shear stress (WSS)	WSS mapping, cross-referenced with	An abnormal WSS pattern has been correlated with	Ultimate understanding of the development and	A detailed vascular geometry is essential for an accurate	20 21 22 25

Continued

CFD in Cardiovascular Medicine - cont

Table 1 Continued

Area	Clinical applications	Data and evidence	Potential clinical impact	Limitations and challenges	References
	vascular disease phenotype, is contributing to the understanding of cellular biology	vascular diseases, including atherosclerosis, aneurysm and post-stent NH	progression of atherosclerosis. WSS map combined with multi-scale modelling may inform clinical practice, such as the site of rupture in aneurysm, and severity of in-stent restenosis.	WSS map. Acquisition of patient specific boundary conditions remains clinically challenging.	
Heart failure	Models based upon CT and MR help compute haemodynamics and the spatio-temporal distributions of pressure and myocardial stress/strain	CFD/FSI models replicate realistic pathophysiology in models of health and disease (eg, HFREF, HFPEF, HCM, DCM, and RWMA post-MI)	Additional haemodynamic data potentially enables early diagnosis and stratifies disease phenotypes and severities. Characterising complex vortex flows identifies areas of flow stagnation and thrombus risk	Resolution of imaging and reconstruction (representing trabeculae and papillary muscles). Tuning with realistic boundary conditions. Requirement for FSI in many models	2 34 35 36 37 38 39 40 41
CRT	Coupled electro-mechanical models of the ventricle incorporating CFD (multi-physics models) used to investigate heart function	Published reports of accurate patient-specific haemodynamic simulations with sufficient detail to optimise CRT before surgical intervention	Improved selection of CRT responders. Simulation and selection of optimal tuning of device settings and lead placement on an individual case basis	Uncertainties and assumptions regarding boundary conditions and the range of clinical measurements required for parameterisation. Mesh generation, prolonged computation times	
VADs	Generic optimisation of pump design. Patient-specific models can aid implantation strategy and tuning of output according to patient physiology	Published models describing haemodynamic influences of catheter placement and minimisation of adverse haemodynamic effects	Pump tuning to ensure periodic opening and closing of AV, preventing leaflet fusion. Personalised catheter placement planning (prediction and avoidance stasis and thrombus formation)	Post-implantation imaging artefact limits modelling. Optimising performance requires the balance of multiple competing factors. As for all cardiac electromechanical models, selection of appropriate patient specific parameters is difficult due to sparsity of data	
Congenital heart disease	CFD simulates haemodynamics which are complex and hard to predict in the context of a diverse and heterogeneous range of disease phenotypes	Range of models described, including reduced order, 3D CFD, FSI and multiscale, particularly in the context of univentricular circulation, aortic and pulmonary malformations	Modelling enables greater understanding of systemic and regional haemodynamics and the prediction of response to putative surgical or device-based treatments which often involve significant modifications to the circulatory tree	Acquisition and application of model parameters and boundary conditions from patient and literature data. The ultimate personalisation challenge	42 43 44

AV, aortic valve; CFD, computational fluid dynamics; CRT, cardiac resynchronisation therapy; CT (A), CT (angiography); DCM, dilated cardiomyopathy; FSI, fluid solid interaction; HCM, hypertrophic cardiomyopathy; HFPEF, heart failure with preserved EF; HFREF, heart failure with reduced EF; MI, myocardial infarction; NH, neointimal hyperplasia; PAP, pulmonary artery pressure; PC, phase-contrast; PCI, percutaneous coronary intervention; RA, regulatory authority; RWMA, regional wall motion abnormality; (v)FFR; (virtual) fractional flow reserve; VAD, ventricular assist device; WSS, wall shear stress.

MODEL CONSTRUCTION

CFD model construction and solution can be described in seven stages (figure 1):

1. Clinical imaging

A range of medical imaging modalities can be used, including ultrasound, CT, MRI and X-ray angiography. Imaging must provide sufficient anatomical and physiological detail, in an appropriate format and quality, to enable segmentation and data extraction.[59]

2. Segmentation and reconstruction

Segmentation methods convert medical images to in silico geometries which define the physical bounds of the model region of interest. If images are acquired over a cardiac cycle, anatomical motion can be tracked over segmented regions.[60 61]

3. Discretisation

Spatial discretisation, or 'meshing', divides the geometry into a number of discrete volumetric elements or cells. Temporal discretisation divides the solution into discrete time steps. The accuracy and numerical stability of the analysis are influenced by both spatial and temporal refinement. The fabrication of the mesh, and the level of mesh refinement, are influenced by case- and context-specific factors. The mesh and timestep (ie, spatio-temporal discretisation) must be refined enough to capture the important haemodynamic behaviour of the modelled compartment (the final solution should be independent of mesh parameters), but without excessive refinement because this impacts negatively on computational resource and solution time (see online supplementary table S1).

4. Boundary conditions

Because it is impossible to discretise the entire cardiovascular system, the region to be analysed will have at least one inlet and one outlet. To enable CFD analysis, the physiological conditions at the wall and inlet/outlet boundaries must be specified. Boundary conditions are a set of applied physiological parameters (which may vary over time) that define the physical conditions at the inlets, outlets and walls. They may be based on patient-specific data, population data, physical models or assumptions.[59]

Youtube video:

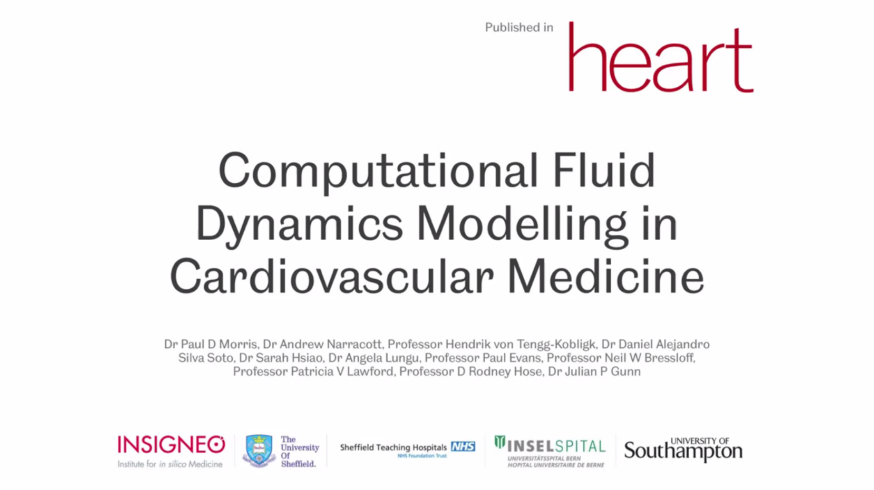

OUTLINE

Part IV

CFD components

CFD Components

1. Mathematical model.
2. Discretization method.
3. Coordinate system.
4. Computational grid.
5. Approximation methodology.
6. Solution method.
7. Convergence criterion.

Mathematical model

- The starting point of any numerical method is, in general, the system of equations and the boundary conditions.
- The choice of the system of equations - e.g. two- or three-dimensional; incompressible or compressible; stationary or unsteady etc. - is related to:
  - Type of problem and application;
  - Information required;
  - Resources - human, instrumental, time - available.
- Usually a solution method has been developed for a particular set of equations.
- A *general* method is impractical (if not impossible) and, like all general-purpose tools, is almost never optimal.

Discretization method - 1/2

- Once the mathematical model has been selected, it is necessary to adopt the most convenient or appropriate discretization method, that is, the method for approximating the differential equations with a system of algebraic equations for the dependent variables, defined on a discrete (finite) set of points in space and time;
- There are many methods in CFD, some of which will be explained later, but the most popular are, in order of diffusion:
  - FVM - *Finite Volume Method*;
  - FEM - *Finite Element Method*;
  - FDM - *Finite Difference Method*.
- Other methods:
  - BEM - *Boundary Element Method*;
  - SEM - *Spectral Element Method*;
  - LBM - *Lattice Boltzmann Method*;
  - DSMC - *Direct Simulation Monte Carlo* method;
  -
  - Particle (mesh-free) methods:
    - VMs - *Vortex Methods*;
    - SPH - *Smooth Particle hydrodynamics*;
    - RBF-FD *Radial Basis Function - Finite Difference*.

  are used in CFD, but their use is often reserved for particular classes of problems, or they are still under active development.

Discretization method - 2/2

- Each discretization method provides the same solution if the grid is *very* (sufficiently) fine.
- However, some methods are more suitable for a certain problem than others.
- The choice of the method is, in industrial reality, linked to:
  - Type of problem.
  - Information required.
  - Previous experience.
  - Personal skills.
  - Availability of software - commercial, in-house or open source.

Coordinate system

- Conservation equations (mass, momentum, energy, etc.) can be expressed in many ways, depending on the coordinate system and vector base:
  - Cartesian
  - Cylindrical
  - Spherical
  - Orthogonal Curvilinear
  - Non-Orthogonal Curvilinear.
- The choice depends on the type of problem, and can influence the discretization method and the grid used.
- The basis with which to define vectors and tensors must also be chosen: fixed or variable, covariant or contravariant, etc.:
  - Depending on this choice, the velocity vector and the stress tensor can be expressed in terms of Cartesian, covariant or contravariant components.
- In the following, unless otherwise specified, we will always use Cartesian components.

Curvilinear coordinate systems - 1/3

- A curvilinear coordinate system (ξ^1, ξ^2, ξ^3) in the space $\mathbf{R}^3$ is defined, with reference to a Cartesian system, by 3 functions of the type:

$$\begin{cases} \xi^1 = \xi^1(x, y, z) \\ \xi^2 = \xi^2(x, y, z) \\ \xi^3 = \xi^3(x, y, z) \end{cases}$$

  or, in tensor notation:

$$\xi^j = \xi^j(x_1, x_2, x_3)$$

- The vector function:

$$\boldsymbol{\xi} : (x_1, x_2, x_3) \rightarrow (\xi^1, \xi^2, \xi^3)$$

  is defined as *change of coordinates*.

- Similarly, the *inverse coordinate change* is defined:

$$\mathbf{r} : \left(\xi^1, \xi^2, \xi^3\right) \rightarrow (x_1, x_2, x_3)$$

- The surfaces of equation $\xi^j = (cost)$ are defined as *coordinate surfaces*. On a coordinate surface only two coordinates vary.
- The 3 lines obtained by intersecting the 3 coordinate surfaces 2 by 2 are called *coordinate lines*. Only one coordinate ξ^j varies along these lines.

Curvilinear coordinate systems - 2/3

- For a generic curvilinear coordinate system ξ^j, the partial derivatives with respect to the Cartesian coordinates can be expressed, by the rules of derivation for composite functions *chain rule*, as a function of the partial derivatives with respect to the curvilinear coordinates.
- If A is a scalar function we have

$$\frac{\partial A}{\partial x_i} = \sum_{j=1}^{3} \frac{\partial A}{\partial \xi^j} \frac{\partial \xi^j}{\partial x_i}$$

and, similarly:

$$\frac{\partial A}{\partial \xi^i} = \sum_{j=1}^{3} \frac{\partial A}{\partial x_j} \frac{\partial x_j}{\partial \xi^i}$$

Curvilinear coordinate systems - 3/3

- Each of the two formulations now seen can be used to relate the Cartesian and curvilinear derivatives of a scalar function A.
- However, there is a difference in the derivatives of the transformation that must be inserted in the relations seen: in the first case it is necessary to evaluate - or approximate - the vectors:

$$\nabla \xi^i \quad (i = 1, 2, 3)$$

while the second requires:

$$\mathbf{r}_{\xi^i} \quad (i = 1, 2, 3)$$

where, for example:

$$\mathbf{r}_{\xi^1} = \frac{\partial x_1}{\partial \xi^1}\mathbf{i} + \frac{\partial x_2}{\partial \xi^1}\mathbf{j} + \frac{\partial x_3}{\partial \xi^1}\mathbf{k}$$

having indicated for convenience with a coordinate reported in the index the partial derivation with respect to that coordinate.

- Therefore all relations involving coordinate transformation must be based on one or the other of the two sets of vectors.

Basis of a vector space

- The basis of a vector space is a set of linearly independent vectors that generate the space.
- Equivalently, each element of the vector space can be expressed uniquely as a linear combination of the vectors belonging to the basis.
- A basis is therefore composed of the minimum number of linearly independent vectors that generate the space.
- The *tangents* to the coordinate lines and the *normals* to the coordinate surfaces represent the *basis* of the cuurvilinear coordinate system.

Covariant basis

- Consider a coordinate line along which only the coordinate ξ^i varies:

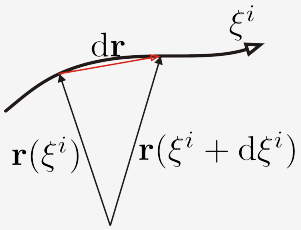

- As is known, the tangent vector to this coordinate line is given by:

$$\mathbf{r}_{\xi^i} = \lim_{\mathrm{d}\xi^i \to 0} \frac{\mathbf{r}(\xi^i + \mathrm{d}\xi^i) - \mathbf{r}(\xi^i)}{\mathrm{d}\xi^i}$$

- These 3 vectors tangent to the three coordinate lines constitute the *covariant* vector basis of the curvilinear coordinate system, and are indicated by:

$$\mathbf{a}_i = \mathbf{r}_{\xi^i} \quad (i = 1, 2, 3)$$

where, as already seen, the three curvilinear coordinates are indicated by ξ^i, $(i = 1, 2, 3)$, and the subscript i indicates the basis vector relative to the coordinate ξ^i, that is, the tangent vector to the coordinate line along which only ξ^i varies.

Contravariant basis

- A normal vector to a coordinate surface on which the coordinate ξ^i is constant is given by $\nabla\xi^i$:

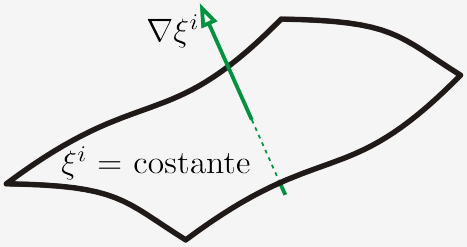

- These 3 vectors normal to the three coordinate surfaces constitute the *contravariant* vector basis of the curvilinear coordinate system, and are indicated by:

$$\mathbf{a}^i = \nabla\xi^i \quad (i = 1, 2, 3)$$

- In this case the index i is indicated as a superscript on the vectors of the *contravariant* basis, in order to distinguish them from the *covariant* vector basis.

Covariant and contravariant basis

- The following figure, showing a six-sided volume element, each side lying on a coordinate surface, illustrates the two basis type:

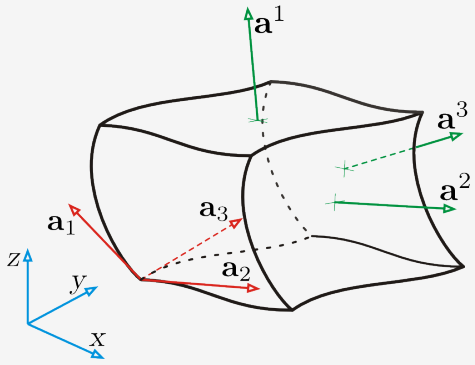

- The following figure shows the decomposition of a generic vector $\mathbf{v}$, for simplicity in the plane, into the *Cartesian* components $\mathbf{v}_i$, into the *covariant* components $\mathbf{u}_i$ and into the *contravariant* components $\mathbf{u}^i$:

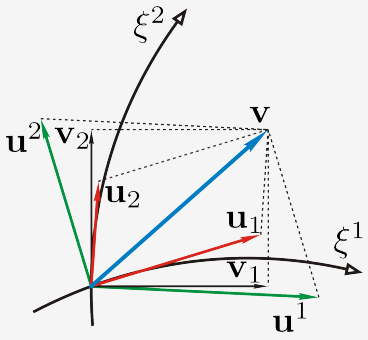

Orthogonal curvilinear coordinate systems

- Only in a *orthogonal* curvilinear coordinate system are the basis vectors of the two systems - covariant and contravariant - parallel, since for a *non-orthogonal* curvilinear coordinate system the normal to a coordinate surface does not necessarily coincide with the tangent to the coordinate line that passes through that surface:

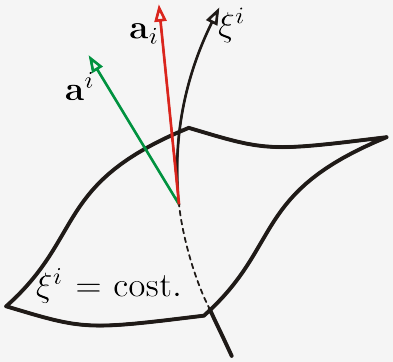

- In an orthogonal curvilinear coordinate system the three basis vectors, of each type, are mutually orthogonal.

Computational grid - 1/5

- The (finite) points at which to calculate the variables are defined by the grid (*grid* or *mesh*), which discretely represents the geometric domain in which the problem is to be solved.
- The most common types of grids are:
  1. Structured (Cartesian, orthogonal and non-orthogonal)
  2. Block-structured
  3. Unstructured.

Computational grid - 2/5

Example of a 2D structured grid around a NACA 0012 airfoil

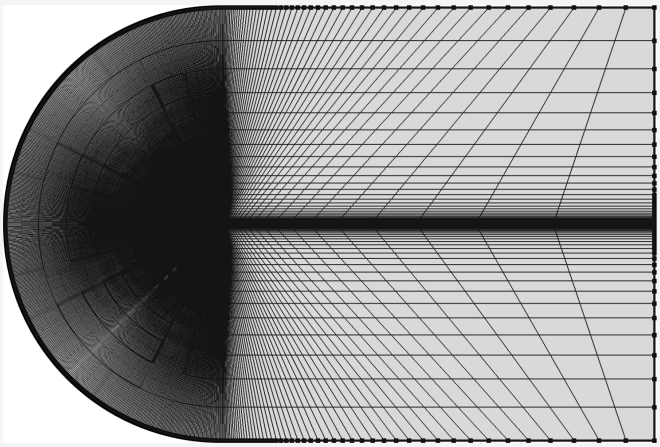

Overall view

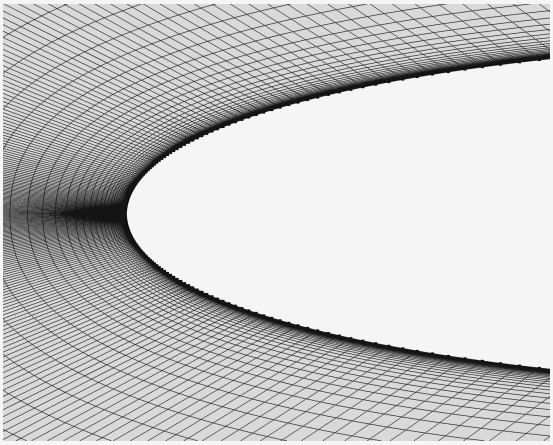

Detail on the leading edge

Computational grid - 3/5

Example of a *overset*-type structured grid (chimera)

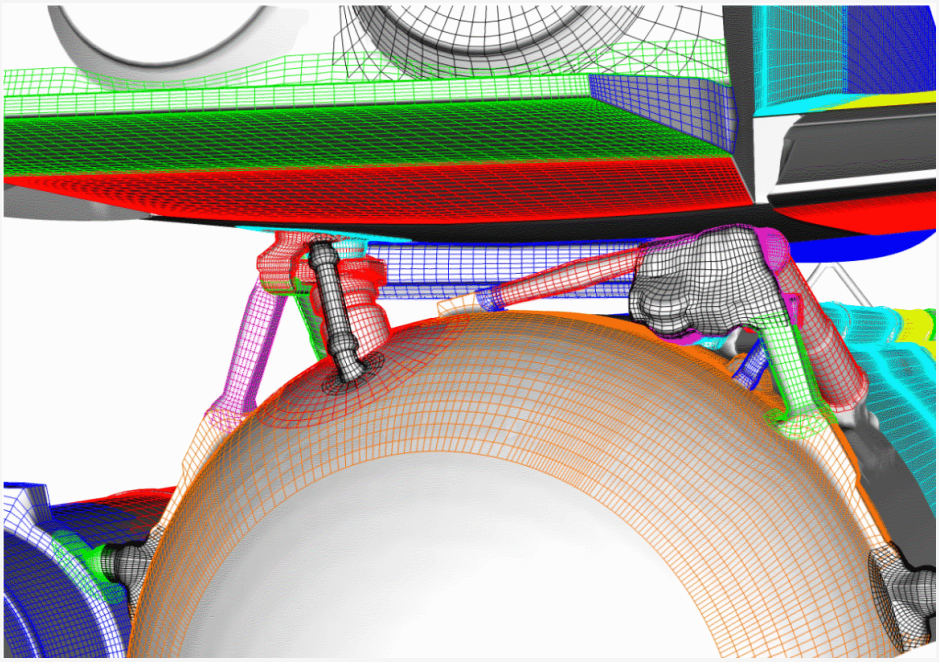

Computational grid - 4/5

Example of an unstructured surface grid

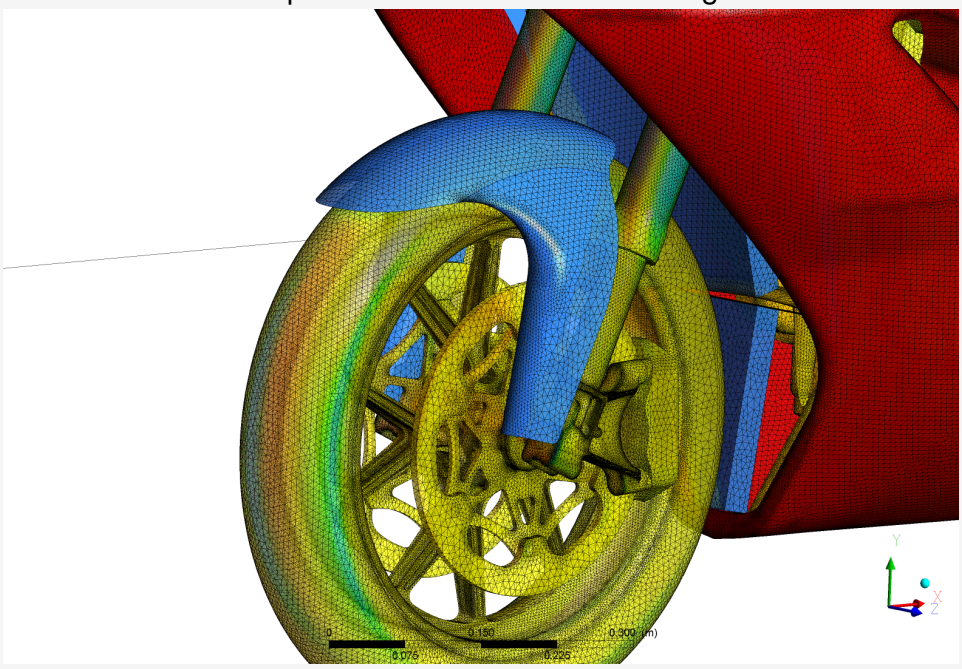

Computational grid - 5/5

Examples of (a) trimmed mesh and (b) polyhedral mesh.

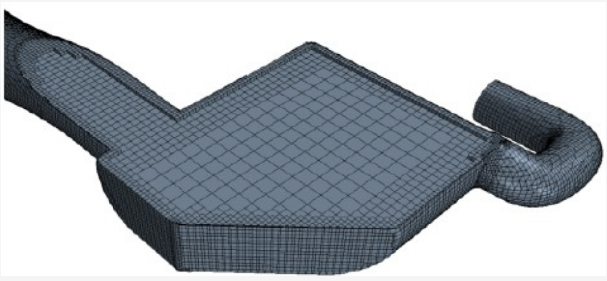

(a)

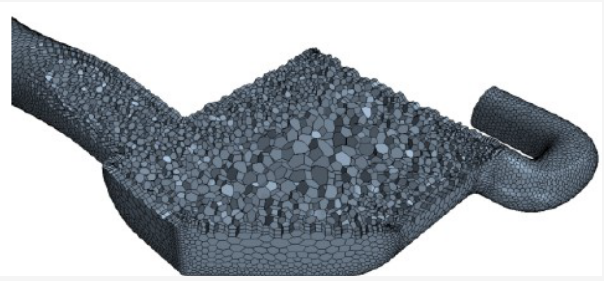

(b)

Approximation method

- After choosing the grid type, it is necessary to choose the approximation(s) used in the discretization:
  - In FDM (Finite Difference Method), the approximations for the derivatives at the grid points must be chosen.
  - In FVM (Finite Volume Method), the interpolation methods (to evaluate the values of the variables at points other than the grid nodes) and the methods to approximate surface and volume integrals must be selected.
  - In FEM (Finite Element Method), the shape functions (elements) and the weighting functions must be chosen.
- There are many possibilities for choice, with important consequences on the accuracy of the solution;
- 2^o order methods often represent a good compromise between accuracy, simplicity and computational efficiency.

Solution method - 1/2

- The discretization usually produces algebraic systems of equations of large size:
  - Such systems can be linear (e.g. explicit or semi-implicit methods) or, more frequently for industrial applications, non-linear. The latter must then be appropriately linearized before proceeding to their solution.
- For non-stationary problems, methods *similar* to those used for initial-value problems described by ordinary differential equations are often used: time-marching:
  - In general, at least for incompressible flows, it is necessary to solve an *elliptic* problem at each time step.
- Stationary problems are frequently addressed - as we will see - by resorting to a sort of time advancement: *pseudo-time marching*, or a similar iterative scheme.

Solution method - 2/2

- Since, as already said, the equations are non-linear, they must be solved *iteratively*, using an appropriate linearization system - *Outer* or *External Iterations*:
  - Such *External Iterations*, moreover, are always necessary when there are non-linearly coupled equations (e.g. turbulence models)
  - The *Outer Iterations* can be interpreted as *distorted* time integration steps, and the solution of the stationary problem corresponds to the asymptotic solution, for $\tau \to \infty$, of the analogous non-stationary problem.
- The linear systems thus obtained are, in general, of large dimension and are usually solved, in the industrial practice, through iterative techniques - *Inner Iterations*;
- The choice of the solution algorithm for the system of linear equations - obtained from linearization - depends on:
  - Grid type
  - Number of nodes/cells
  - Equation type (pressure correction, momentum, turbulent kinetic energy, etc.).

Convergence criteria

- Using iterative methods, it is necessary to establish the *convergence criteria*, that is, to define the limit values of some quantities - convergence indicators - beyond which it is useless, and/or expensive, to continue with the iterations:
  - *Outer* iterations: necessary due to the non-linearity and coupling of the equations;
  - *Inner* iterations: used to solve linear systems of equations.

OUTLINE

Part V

CFD workflow

Classical CFD workflow

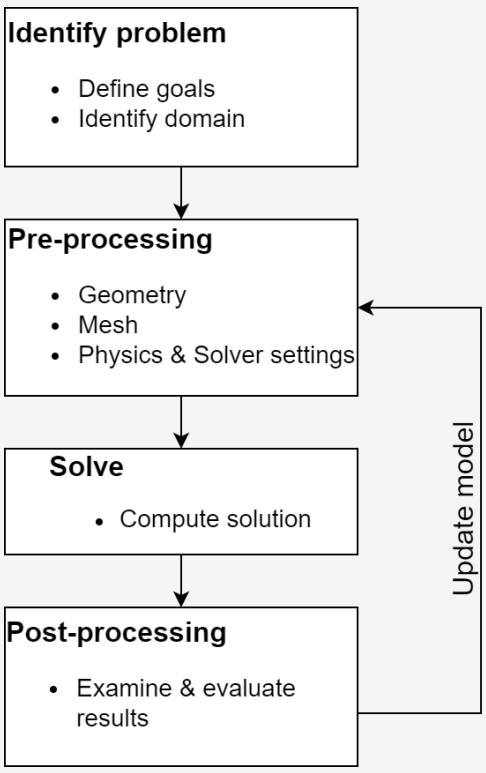

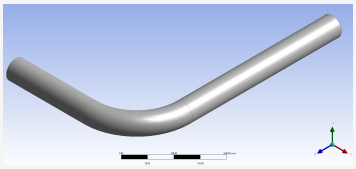

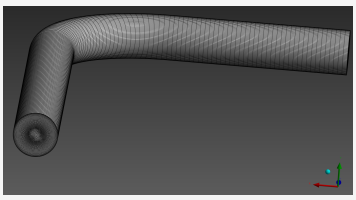

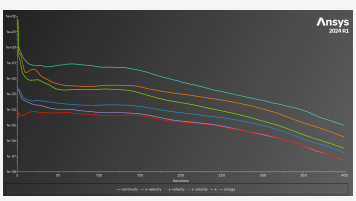

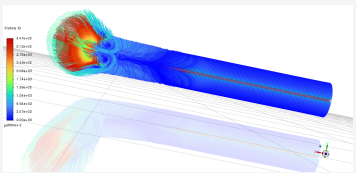

Modeling goals

- What results are required, e.g. pressure drop, mass flow rate, heat flux, lift force et.
- What modeling options and semplifications are deem acceptable?
  - What simplifying assumptions can/must be made, e.g. steady-state, 2D, symmetry, periodicity, et.
  - What physical models must be included in the analysis (turbulence, heat transfer, free surface et.)
- What degree of accuracy is required ?
- How many resources (time, computing platforms, man-hours) are available?
- Is CFD an *appropriate* tool at this stage?

Choice of Domain and mesh resolution

- How you select the part/component of the system to analyze?
- Are boundary conditions available?
- Can it be approximated as e.g. 2D or axi-symmetric ?
- How will you obtain a model of the *fluid* region?
  - Use an existing CAD model?
  - Extract the *fluid* region from a solid part?
  - Create from scratch?

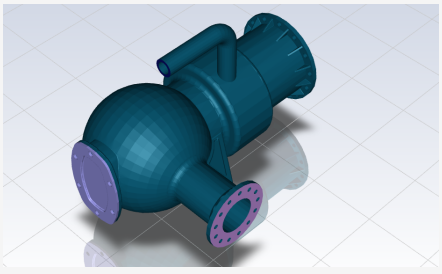

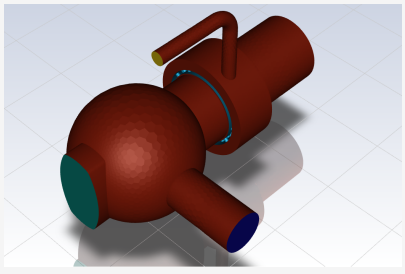

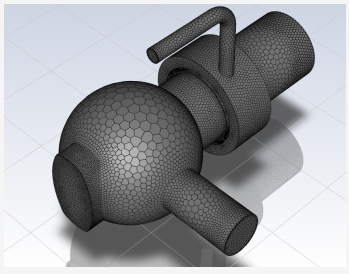

- What is the required mesh resolution?
- Are adequate computational resources available?

Computing the solution

- The discrete equations are solved iteratively until convergence
- Convergence is reached when:
  - Residuals are below a specified tolerance, *e.g.* 1×10^{-5}
  - Overall conservation is achieved, e.g. mass flow in = mass flow out
  - Quantities of interest - lift, drag. heat flux, force et. - do not change anymore
- The accuracy of a solution is dependent upon:
  - Degree of convergence
  - Mesh independence
  - Appropriateness of mathematical (physical) model

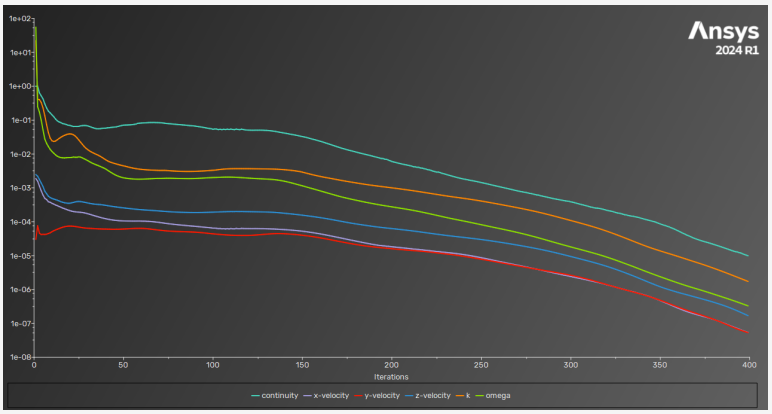

Examine the results and review the model

- Examine the results:
  - What is the overall flow pattern?
  - Is there separation/reattachment?
  - Is the heat flux uniformly distributed?
  - Are the most important flow features adequately resolved?

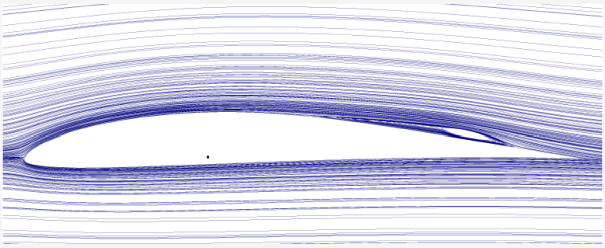

- Evaluate quantitative results:
  - Flow rate, pressure drop
  - Forces (drag, lift), moments
  - Average heat transfer coefficients
  - Highest temperature
  - Surface/volume integrated/averaged quantities
- Are the physical models appropriate. e.g. laminar/turbulent, steady/unsteady et.
- Is the computational domain adequate?
- Are boundary conditions correct?
- Is the mesh adequate, *e.g* does the model contains (some) poor quality cells?

OUTLINE

Part VI

Numerical Methods in CFD

Consistency

- The discretization should provide the *exact* value when the size of the grid - spatial and temporal - tends to zero.
- The difference between the discretized equation and the exact one is called *truncation error*:
  - Estimated by replacing the nodal values ??in the discrete approximation with a Taylor series expansion (we will see some examples when talking about *Finite Differences*);
  - The result is the original differential equation plus a *remainder*, which represents the truncation error.
- For a method to be considered *consistent*, the truncation error must become zero as the grid size approaches zero: $\Delta x_i \to 0$ and $\Delta \vartheta \to 0$.
- The truncation error is usually proportional to a power of Δx_i and/or $\Delta \vartheta$:
  - ➢ Δx_i^n n order method ($n > 0$) in space (n-th order spatial accuracy);
  - ➢ $\Delta \vartheta^m$ m order method ($m > 0$) in time (m-th order time accuracy).
- Ideally, all terms of the equation should be discretized with approximations of the same order, but in some cases it is preferable to treat the dominant terms more accurately (e.g. convective terms for flows at high Reynolds number).
- Even if the approximation is consistent, this does not guarantee, in general, that the solution of the discretized equation will become equal to the exact one for $\Delta x_i \to 0$: the solution method must be *stable*.

Stability

- In a simple way, we can define *Stable* a numerical solution method that *does not amplify* the errors that (inevitably) appear during the solution:
  - For iterative methods, a *stable method* is a method that *does not diverge*;
  - For nonstationary problems, stability guarantees that the method provides a *bounded* solution when the exact solution of the equation is *bounded*.
- Stability is difficult to quantify, especially for nonlinear problems with realistic boundary conditions:
  - Simplified approach: linear problems with constant coefficients in the absence of boundary conditions.
- The most widely used approach in the study of stability is the *Von Neumann* method;
- When dealing with complex problems, typical of the industrial sector, with coupled non-linear equations and complex boundary conditions, it is not easy to establish the stability criteria:
  - Upper limit on the time step (even for purely implicit methods);
  - Need for under-relaxation;
  - ...
  - Experience and intuition !

Convergence

- A numerical method is defined as convergent if the solution of the discretized equations *tends* to the exact solution (of the differential equation) when $\Delta x_i \to 0$;
- Convergence *is not* synonymous with consistency;
- For linear initial value problems, the *Lax equivalence theorem* (Richtmyer and Morton, 1967), states that:

Theorem

For a well-posed linear initial value problem and a finite difference approximation satisfying the consistency condition, the latter is convergent if and only if it is stable.

- A consistent, but unstable, method is *non* convergent and, as such, is useless;
- In practice, convergence is determined on the basis of numerical experiments on increasingly finer grids:
  - *Grid-independent* solution;
  - For *sufficiently fine* grids, the degree of convergence is determined by the truncation order;
  - Estimation of the error in the solution.

Conservation

- The equations to be solved are *conservation equations* (see *Introduction to the laws of fluid motion*), so the numerical methods used should respect - globally and locally - these laws:
  - Under steady-state, source-free conditions, the amount of a quantity, such as mass, leaving a closed volume must equal the amount entering.
- By using the equations in the conservative (divergence) form, and adopting the *Finite Volume Method (FVM)*, the conservation is guaranteed on a local (Finite Volume) and global (entire domain) basis;
- Other methods, such as the Finite Element Method (FEM), can also be made conservative;
- The treatment of source terms must be consistent, so that the total amount of a quantity generated (source) or absorbed (sink) in the domain is equal to the net flux of the same quantity through the boundary of the domain itself;
- The conservation is a fundamental property, as it imposes a constraint/limit on the error of the solution.

Boundedness and realizability

Boundedness

- The numerical solutions should remain within appropriate limits:
  - Non-negative quantities – e.g. density, turbulent kinetic energy – should always remain positive, possibly even during intermediate iterations;
  - Quantities, such as concentrations, should be between 0 and 1 (0% - 100%);
  - In the absence of sources, temperatures must be between those of the boundaries.

Realizability

- Models of phenomena too complex to be addressed directly, e.g. turbulence, combustion, multiphase flows, etc., must yield physically realistic solutions.

Realizability example

The realizable $k-\varepsilon$ model

Most commercial (industrial) and open source CFD packages now offer, beyond the standard $k-\varepsilon$ two-equation turbulence model, the so-called *realizable* k-ϵ *model*. This model differs from the standard k-ε model in two ways:

1. It contains a new formulation for the turbulent viscosity.
2. A new transport equation for the dissipation rate, ε, has been derived from an exact equation for the transport of the mean-square vorticity fluctuation.

The term *realizable* means that the model satisfies certain mathematical constraints on the *Reynolds stresses*, consistent with the physics of turbulent flows. Neither the standard $k-\varepsilon$ model nor the RNG $k-\varepsilon$ model is *realizable*.
The Boussinesq hypothesis relates the Reynolds stresses to the mean velocity gradients by means of the *turbulent viscosity* μ_t:

$$-\rho\overline{u_i' u_j'} = \mu_t \left(\frac{\partial u_i}{\partial x_j} + \frac{\partial u_j}{\partial x_i} \right) - \frac{2}{3} \left(\rho k + \mu_t \frac{\partial u_k}{\partial x_k} \right) \delta_{ij}$$

where μ_t is computed by combining k and ε as follows:

$$\mu_t = \rho C_\mu \frac{k^2}{\varepsilon}$$

Combining both equations we obtain the following expression for the *normal Reynolds stress* in an incompressible strained mean flow ($\nu_t = \mu_t/\rho$):

$$\overline{u^2} = \frac{2}{3}k - 2\,\nu_t \frac{\partial U}{\partial x}$$

It results that the normal stress, $\overline{u^2}$, which by definition is a positive quantity, becomes negative, i.e., *non-realizable*, when the strain is large enough to satisfy:

$$\frac{k}{\epsilon}\frac{\partial U}{\partial x} > \frac{1}{3C_\mu} \approx 3.7$$

Accuracy - 1/2

- Numerical fluid dynamics methodologies always give rise to *approximate solutions*;
- Apart from any errors introduced in the *set-up* phase (programming errors - bugs - incorrect choice of the solution algorithm, incorrect boundary conditions etc.), the solution is always affected by *three types of systematic errors*:

  Modeling errors: difference between the *real problem* and the *exact solution of the mathematical model*. These errors are due, for example, to the assumptions underlying the problem (stationarity or not; 2D or 3D; possible periodicity, etc.), to the choice of the calculation domain, to the choice of the turbulence model, to the boundary conditions, to the limited knowledge of the thermophysical properties, to the choice of possible multiphase models, to the choice of the combustion model, etc.;

  Discretization errors: difference between the *exact solution of the equations (mathematical model)* and the *exact solution of the systems of equations* obtained with the discretization. It decreases as the grid refinement increases;

  Convergence errors: difference between the *exact solution of the systems of equations* obtained as a result of the discretization, and the *solution obtained through iterative algorithms*. It decreases as the number of iterations increases.

Accuracy - 2/2

- It is particularly important to take these errors into account, and above all to be able to distinguish them;
- Some errors may be dominant, and sometimes assume the same value and opposite sign, with the consequence of giving rise, for example, to apparent greater accuracy with simulations performed on coarser grids;
- In order to establish any modeling errors, it is first necessary to fully verify, and minimize, the convergence and discretization errors;
- There are various ways to numerically address a thermofluid dynamics problem, but it is important to remember that, in applications, the goal is often to obtain the desired accuracy with the minimum effort, or - more frequently - the maximum accuracy with the available resources.